Machine Learning Applications for Dynamic Security Assessment in presence of Renewable Generation and Load Induced Variability

By

Anubhav Nath

A Thesis presented in Partial Fulfillment
of the Requirements for the Degree
Master of Science

Approved April 2019 by the
Graduate Supervisory Committee:

Anamitra Pal, Chair
Keith E. Holbert
Meng Wu

ARIZONA STATE UNIVERSITY
May 2019

ABSTRACT

Large-scale blackouts that have occurred across North America in the past few decades have paved the path for substantial amount of research in the field of security assessment of the grid. With the aid of advanced technology such as phasor measurement units (PMUs), considerable work has been done involving voltage stability analysis and power system dynamic behavior analysis to ensure security and reliability of the grid. Online dynamic security assessment (DSA) analysis has been developed and applied in several power system control centers. Existing applications of DSA are limited by the assumption of simplistic load profiles, which often considers a normative day to represent an entire year. To overcome these aforementioned challenges, this research developed a novel DSA scheme to provide security prediction in real-time for load profiles corresponding to different seasons. The major contributions of this research are to (1) develop a DSA scheme incorporated with PMU data, (2) consider a comprehensive seasonal load profile, (3) account for varying penetrations of renewable generation, and (4) compare the accuracy of different machine learning (ML) algorithms for DSA. The ML algorithms that will be the focus of this study include decision trees (DTs), support vector machines (SVMs), random forests (RFs), and multilayer neural networks (MLNNs).

This thesis describes the development of a novel DSA scheme using synchrophasor measurements that accounts for the load variability occurring across different seasons in a year. Different amounts of solar generation have also been incorporated in this study to account for increasing percentage of renewables in the modern grid. To account for the security of the operating conditions different ML algorithms have been trained and tested. A database of cases for different operating conditions has been developed offline that contains secure as well as insecure cases, and the ML models have been trained to classify the security or insecurity of a

particular operating condition in real-time. Multiple scenarios are generated every 15 minutes for different seasons and stored in the database. The performance of this approach is tested on the IEEE-118 bus system.

To my parents

ACKNOWLEDGEMENTS

I take this opportunity to express my sincere gratitude towards my advisor Dr. Anamitra Pal who has supported and guided me throughout the course of this research work. I had always dreamt of writing a thesis as a part of my master's degree and I am thankful to him for giving me an opportunity to work under his supervision.

I would like to thank my committee members Dr. Keith E. Holbert and Dr. Meng Wu for taking their time out to be on my thesis committee and for their valuable inputs.

And finally, I would like to express my deepest gratitude towards my family members for their relentless support and encouragement. I am also thankful to my friends and anyone who has directly or indirectly extended their help in completion of this thesis.

TABLE OF CONTENTS

Page

CHAPTER Page

CHAPTER Page

LIST OF TABLES

Table Page

Table Page

LIST OF FIGURES

Figure Page

CHAPTER 1

1. INTRODUCTION

1.1 History of Electricity

In modern day world very few other inventions is as important as the invention of electricity. Even before we started harnessing the power of electricity-*it has been used in nature by electric fishes such as eels and catfish.* Ancient cultures in the Mediterranean and the Greeks made observations of static electricity by rubbing amber with cat fur that could attract light objects like feathers. The great inventor Benjamin Franklin was the first person to conduct the most famous experiment of flying a kite, having a key made of metal attached to the string during a thunderstorm in order to route electricity. In 1831, another great inventor Michael Faraday created the very first electrical generator with the use of moving coils made of copper through a generated magnetic field. This was the first instance of creation of electricity. Thomas Edison later perfected the work of Faraday and created the first generator model which could be used to supply electricity. In the decades to follow, inventors like Tesla, Westinghouse, and Oersted paved the path for use of electricity as we know it today. Electricity is one of the greatest inventions of all time as it paved the way to inventions which now drive the world to a better place with implications on socio-economic human development.

1.2 Requirements of a reliable electric power supply

In modern day world we depend on electricity unlike any other invention. Human civilizations around the world depend on a continuous and reliable supply of electricity for day to day activities and progress of the economy. This high dependency on electricity has led the electrical grid operators to work more carefully in order to ensure a very reliable supply of electricity. During the North American blackout of 2003, approximately 50 million people were affected in the north

eastern states of American and parts of Canada. The blackout was prevalent for up to 4 days in certain areas and the economic impact was about $4 billion to $10 billion [1].A joint task force was developed to investigate the cause of this blackout and it was found out that there was a lack of situational awareness in the grid and there was a need for better reliable tools to monitor the grid [1]. With the growth of an interconnected power system and the trend to move towards achieving an electrical supply which would have higher amount of renewable generation [2] it is of utmost importance to maintain a reliable supply in the grid. It has been stated in [3], that smart grids should have the capability of accessing transient and voltage stability in real time for better monitoring, control and protection. One of the key aspects of this work has been to highlight the importance of synchrophasor technology in today's grid. The gradual change of the utilities to move towards the use of phasor measurement units (PMUs) for monitoring and visualization instead of supervisory control and data acquisition (SCADA)-based framework have been duly highlighted. The role of synchrophasor technology in real time wide area monitoring applications have been shown in [4],[5] and also its use in preventive control have been duly studied in [6],[7]and [8].A committee was set up by IEEE to come up with a comprehensive definition of power system security in which aspects of power system security have been clarified. In [9], the definitions pertaining to a secure power system was formulated wherein under any disturbance the power system should be able to:

1) Survive transient instability condition and thereby attain steady state operating condition.

2) After attaining steady state condition, both the voltage and the frequency of the power system should be within operable limits.

Furthermore, North American Reliability Council (NERC) in 1997 [10] had proposed the definition of power system security as the - *ability of the bulk power electric system to withstand*

sudden disturbances such as electric short circuits or unanticipated loss of system components.

1.3 Dynamic Security Assessment (DSA) Scheme

The power system of the modern world demands a much improved situational awareness scheme in order to enable the operator to have a better visualization of the entire system for any contingencies that might advertently affect the system. DSA is designed to solve this problem. Kundur in his paper [11] defines DSA as follows:

"*DSA refers to the analysis required to determine whether or not a power system can meet specified reliability and security criteria in both transient and steady-state time frames for all credible contingencies."*

Due to the growing complexity of the power system with the addition of large amounts of renewable generation in the grid, it has become a necessity for system operators to operate the system at near stability limits. Offline security assessment tools are not reliable in this aspect and thus the need of a better online real time security assessment tool has been stressed further. With the growth of synchrophasor technology, utilities around the world have started to harness the power of real time visualization that can be provided by the sensors that are placed in the grid. In 2007, the CIGRÉ working group published a report [12] in which it highlights the importance of DSA schemes on today's grid. Savulescu in his book [13] gave a detailed description of the structure of a DSA scheme which has been shown below in Fig. 1.1.

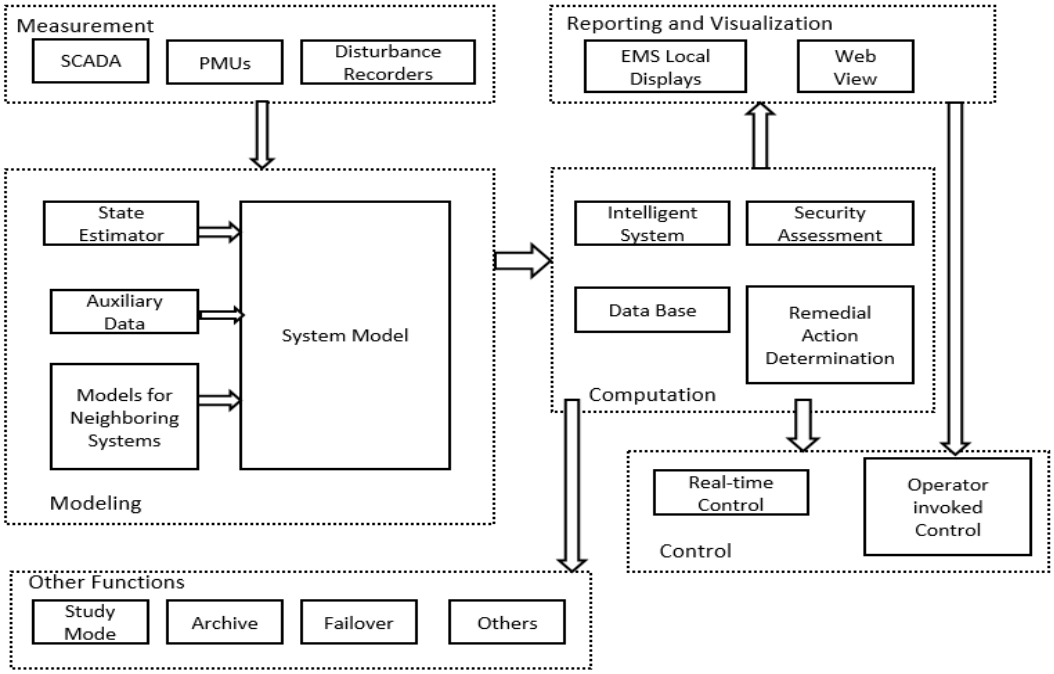

Figure 1. 1 Components of a DSA and their interaction [13][13].

Challenges pertaining to online DSA scheme is to measure the current stability condition wherein margins of the secure/insecure regions are fundamentally important to the system operators. Different conditions of stability needs to be studied in order to determine the security of a region- rotor angle stability, frequency stability, transient stability ,small signal stability and short term voltage stability. The power system operator in real time can take preventive control actions in order to prevent a cascading blackout that can cause power loss in a large section of the grid.

1.4 Phasor Measurement Unit (PMU)

A phasor measurement unit (PMU) is a device which is used to estimate the magnitude and phase angle of an electrical phasor quantity like voltage and current and which is accurately time synchronized using GPS. It has been stated in IEEE Standard for Synchrophasor Measurements for Power Systems [14] that the frequency error for PMU is limited to 0.005 Hz, while the total vector error (TVE) should be less than or equal to 1%.PMUs have the capability to send and receive communication packages from data concentrators across the grid and can give better visualization

and control capability to the system operator. PMUs have been used in a wide area of research, some of which have been presented in [15]-[20].In the United States about 2,500 PMUs have been installed across the power network by the end of 2017 [21].

1.5 Literature Review

The introduction of dynamic security assessment (DSA) scheme first started around the 1960's when the first major blackout happened on November 9, 1965 in the north eastern part of United States [22]. The blackout affected roughly 30 million people whose supply to electricity was cut off for around 13 hours. The cause of the failure was mis-operation of a backup protection relay on one of the major transmission lines between the United States and Canada. This caused a major rerouting of power along the other transmission lines which led to a cascading failure.

DSA mainly deals with rotor angle stability or transient stability and does an assessment of the power system's ability to maintain synchronism when the system is experiencing sudden disturbance such as loss of load, stalling of generator or short circuit on a transmission line [23].In power system planning studies, transient stability is carried out to determine the robustness of the system by utilities .However the methods such as numerical integration that goes into conducting of such studies is time consuming and computationally very taxing. Thus, while doing a security assessment, it is omitted out from the process involved in it [24],[25].Due to this, there was a necessity to use direct transient stability assessment based methods which were based on Lyapunov method [26].

Direct methods for transient stability assessment have been proposed by Athay in [27] and subsequently by Fouad in [28] . Xue in [29] came up with a simpler and fast method for calculating stability under practical constraints. These methods would use an energy function based method to determine the stability of the system by comparing the system conditions to a critical value

before and after a fault has occurred.

Khorasani in [30] used a physically based decomposition technique to perform direct stability analysis of the power system model using an energy function approach. In [31],Chiang used a method called boundary of stability region based controlling unstable equilibrium point method (BCU method),to do a dynamic contingency screening .The design objective of such a classifier was formulated to ensure that the single or multi swing contingencies are completely captured and the number of contingencies needed to determine for further analysis is greatly reduced.

Beside the above mentioned methods which involve numerical integration and energy function, methods such as probabilistic methods, dynamic state estimation and data mining methods have also gained popularity while performing DSA scheme. Dynamic state estimation has been performed by Jain in [32] which uses a tracking state estimation algorithm. Tracking state estimation provides a fast and real time update on the state of the power system without any physical modeling of the time varying nature of the system. Valverde in [33] proposed an unscented Kalman filter based dynamic state estimator. In this method, the constraints of highly nonlinear mathematical model of power systems is overcome by using the unscented transformation which leads to a better accuracy with a simpler implementation model.

Probabilistic techniques used for DSA scheme takes into account varying system conditions and states while determining the security of a region. An analytical approach to DSA scheme of power system while incorporating wind farms was proposed in [34] .The probability of transient stability index given a specific fault and uncertainties of wind power output was calculated analytically based on practical dynamic security of the region with doubly fed induction generator and Cornish-Fisher expansion. Dissanayaka in [35] proposed a linearized technique to determine a risk based index for DSA. Risk based approach in this study incorporated the probability of operating

conditions and contingencies and constructed the system risk at any given moment.

With the advent of PMUs in the grid, a large amount of data is available for better analysis of the system states. Data mining techniques can be successfully adopted to deal with the large amount of data available by employing proper learning methods. In [36], the reasons to shift from offline to online security assessment has been described, which is summarized below:

- Industry trends have adversely affected system dynamic performance. A power network which is under stress has a substantially different response than that of a non-stressed system. Offline methods tend to be conservative when determining the available power-transfer ability which might hamper the system security.
- The potential size and effect of contingencies have increased dramatically .When a power system is operating close to its limit, a relatively smaller disturbance might cause the system security to be violated.
- Certain scenarios which are encountered in the system cannot be anticipated beforehand. Thereby using an off-line based study might prove to be fatal in such a condition.

With the shift to an online based security assessment it is of further importance to employ better machine learning models or data mining methods to determine security of the system. Data mining techniques or the use of machine learning (ML) algorithms are seen to have certain features that can bring benefits to the real-time environment:

- Data mining models are computationally very fast. With the introduction of large CPU computing systems, learning algorithms acts very quickly and can analyze the behavior of a system in real time.
- The ML methods can quickly learn the system states due to its use of intelligent algorithms.

- ML algorithms can discover hidden traits present in the data which was previously unknown to the observer and thus increase the system observability.
- Data mining methods tend to have the ability to process large sets of data (PMU/ SCADA) into more meaningful and manageable information for the system operator.

Huang in [37] developed an intelligent system technique using pattern recognition techniques along with the use of KNN predictive models interfaced with existing system models. It provided a method to automatically compute security limits online with the help of state estimator models considering all possible contingencies and transactions. In [38] , a DSA scheme is developed which takes into consideration large penetration of wind power. The research proposed a data mining framework for real time DSA scheme which consisted of a DSA engine whose role is to perform real time DSA, a wind power and load demand forecasting engine for prediction of offline and online wind power generation, a database generation scheme for training the data mining method and a model updating engine for updating of online DSA. Decision Tree (DT) is one of the most popular data mining method used for DSA. Sun in [39] proposed the use of DT to perform a DSA scheme. The proposed scheme built and updated DTs offline to decide critical attributes as the security indicators. DT based preventive and corrective applications for DSA was proposed in [40]. Preventive and corrective controls such as generation rescheduling and load shedding schemes were developed based on the security regions and boundary conditions. Support Vector Machine (SVM) has been used in [41] to determine security assessment of a system. Least squares based SVM have been proposed in this study and is compared with multilayer neural networks to test its efficiency. In [42], the authors adopted a binary SVM based method to determine transient security. Extreme learning machine (ELM) is another type of learning algorithm which have been duly employed in [43] to determine real time DSA scheme. Random forest (RF) has been utilized

in [44] to better classify the security status of the DSA scheme.

In 2007, CIGRÉ Working Group C4.601 published an extensive review of online DSA tools and techniques [45]. The report was a reflection of the current trends and practices in the field of online DSA. Table 1.1 provides a list of the installations of DSA scheme worldwide. The table provides information on the varying assessment methods where the following terms are presented, TSA stands for transient security assessment, VSA for voltage security assessment, SSA for small signal security assessment, and FSA for frequency security assessment. The last column provides a view of the status of installation where I/S is referred as “in service”, O/S to “tested but out-of-service” and U/D is referred as “under development”.

Real time DSA scheme can be categorized into following two categories: post-fault DSA and pre-fault DSA. Post-fault DSA scheme is triggered when the system is able to detect a fault in the system and immediate stability analysis is carried on thereafter. However this system fails to work if a fault was undetected in the system which might have severe consequences in the system. Pre-fault DSA is employed much before a fault is occurred and as such this method is capable of mitigating the risk of cascading blackouts by alerting the system operator of possible preventive control actions that needs to be undertaken. DSA scheme with pre-fault capability is thus the need of the hour in modern day power system.

Table 1. 1: State of the art Dynamic Security Installation [45]

Country	Location/Company/Project	Scope				Status
		TSA	VSA	SSA	FSA	
Australia	NEMMCO	x		x (MB*)	x	I/S
Bosnia	NOS	x	x			I/S
Brazil	ONS	x	x	x	x	I/S
Canada	BCTC	x	x			U/D
Canada	Hydro-Quebec	x	x			I/S
China	Beijing Electric Power	x				I/S
China	CEPRI	x				I/S
China	Guangxi Electric Power	x		x	x	I/S
Finland	Fingrid		x	x (MB*)		I/S
Greece	Hellenic Power System		x			I/S
Ireland	ESB	x	x			I/S
Italy and Greece	Omases Project	x	x			O/S
Japan	TEPCO	x	x			I/S
Malaysia	Tenaga Nasional Berhad	x	x			I/S
New Zealand	Transpower	x	x		x	I/S
Panama	ETESA	x	x			I/S
Romania	Transelectrica	x	x			I/S
Russia	Unif.Elect.Power System	x	x			I/S
Saudi Arabia	SEC	x	x			U/D
South Africa	ESKOM	x	x			U/D
USA	PJM	x	x	x		I/S
USA	Southern Company	x				I/S
USA	Northern States Power	x				I/S
USA	MidWest ISO		x			I/S
USA	Entergy		x			I/S
USA	ERCOT	x	x			I/S
USA	FirstEnergy		x			U/D
USA	BPA		x			I/S
USA	PG&E		x			U/D
USA	Southern California Edison		x			U/D

* MB: Measurement Based

1.6 Limitations of Existing Studies

All the above-mentioned studies [28-38] have neglected the load variations that can occur in a particular season of a year. To conduct DSA, heavy or light loading conditions of a season is often selected which may not best represent the varying load profiles that can occur in different seasons. Furthermore, from CAISO (California ISO) open source database we can visualize that seasonal load profiles are different for each particular season. The load variability in a particular season

should therefore be taken into account to perform DSA to account for any misclassification in security states that can occur in different seasons. With an increasing amount of renewable generation in the network, it is of utmost importance to simultaneously incorporate varying levels of renewable penetration to better qualify the security of a system. These two knowledge gaps identified in the literature survey are addressed in the research conducted in this thesis using different ML techniques.

1.7 Overview of the Thesis

The thesis has been organized as described below:

- Chapter 1 is an introductory chapter that outlines the background and related work as well as the limitations of the existing studies for performing online DSA.
- Chapter 2 explains the methodology of the proposed DSA scheme, optimal PMU placement in the grid, and security criterion chosen for the study.
- Chapter 3 gives an overview of the different ML techniques that have been used as a part of this research. The structure of the algorithms with proper explanation of their working methodology have been provided.
- Chapter 4 describes the simulation setup, database generation for different load profiles, and performance comparison of the proposed DSA scheme using different ML Techniques.
- Chapter 5 concludes the conducted research and outlines some of the steps that can be considered in the future.

CHAPTER 2

2. DYNAMIC SECURITY ASSESSMENT SCHEME

2.1 Introduction to Proposed Dynamic Security Assessment (DSA) Scheme

DSA plays an important role in determining the security of the power system in real-time. It assists the power system operator in operational decision-making and initiating remedial control processes. The flowchart for the proposed ML based online DSA scheme is shown in Fig. 2.1.

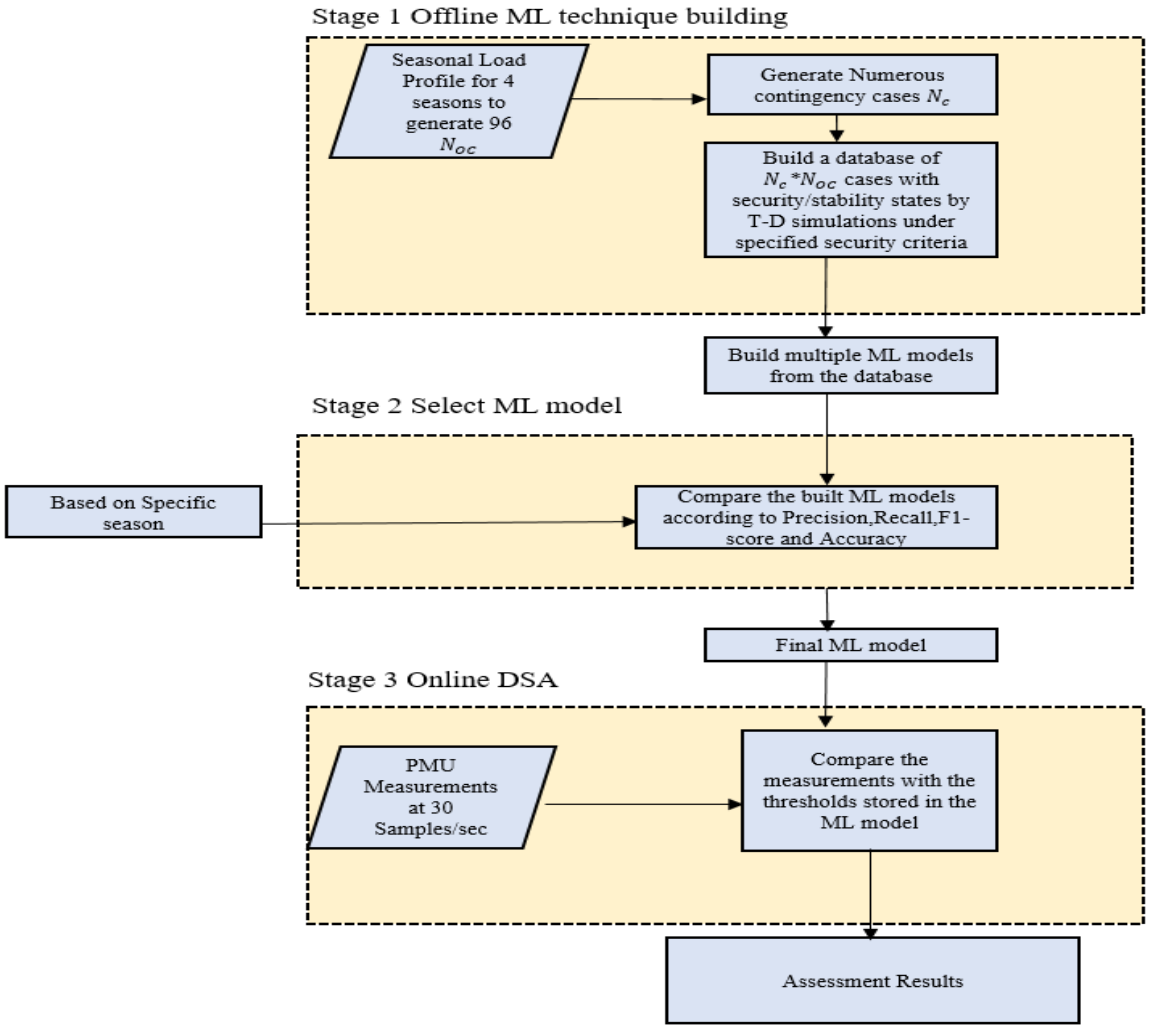

Figure 2. 1 The flowchart for the ML based online DSA scheme

The proposed approach is executed in the following three stages.

Stage 1: Offline ML technique building

In this stage, multiple operating conditions,N_{oc} are generated on a seasonal based load profile. Corresponding to 4 different seasons in a year, each load profile will have multiple number of N_{oc}. Industrial standards demand that OPF must be performed in an interval of (at least) every 15 minutes throughout the day. Considering this timeframe, the N_{oc} selected for each normative seasonal load profile on a 15-minute interval basis comes out to be 96.

The next task is to select the number of critical contingencies, N_C for generating the database. N_C contingencies based on types, locations, fault durations, etc. are typically selected by the operator from a history of critical contingencies. For each N_{oc}, detailed time domain simulation (TDS) of all the N_C contingencies are executed. Specified security criteria, dealing with transient stability and short-term voltage security, are then checked to determine the security classification for each case. The classifications may be binary i.e. "secure" (if no criterion is violated) or "insecure" (otherwise) or "multiple", e.g., transient instability, short term voltage insecurity, insufficient damping, frequency insecurity, etc., with different priorities assigned to each criterion. In this study, the classification parameter has been selected to be binary ("1" for a secure case and "0" for an insecure case).

Finally, a database of $N_{oc} * N_C$ cases each including a security classification and a vector of predicted values is generated and further divided into a learning or training set and a testing set. The percentage of training set of the entire database is 70% while the testing set comprises of 30% of the entire database. Different ML algorithms are thereby trained on the created database for each season to create the trained model for each of the applied algorithm, namely, decision tree (DT), random forest (RF), support vector machine (SVM), and multi-layer neural network

(MLNN). For each seasonal load profile, the number of critical contingencies N_C has been chosen to be 50. '$N-1$' contingencies and multiple '$N-k$' contingencies are simulated to create the secure and insecure cases. The simulation length for each contingency and corresponding to each operating condition is 20 seconds where the first contingency is executed at the 5th second and '$N-k$' contingencies (for $k \geq 2$) have also been executed at the 5th second.

Stage 2: Select the ML model

In this stage a ML model is selected which is optimal for the specified season. Based on the four seasons (summer, fall, winter, and spring), the ML model needs to be selected which will be subsequently feed into the online DSA scheme. The performance classifiers for each of the ML models will be tested to guarantee optimal classifying ability for each of the algorithms. Performance classifiers such as precision, recall, f1-score, and accuracy are cross-validated across the built ML models to find out the best model. The simulations are repeated a number of times and a 95% confidence interval accuracy was selected to account for the deviation in the performance classifiers of each of the ML algorithms.

Stage 3: Online DSA

In real-time, the control centers obtain synchronized measurements from the Wide Area Measurement System (WAMS)-sensors, namely PMUs, to perform DSA for either single or multiple contingencies. Control centers can obtain measurements from SCADA, PMU, or a hybrid measurement system comprising of both PMU and SCADA. In this study, it has been assumed that the online measurements are obtained from PMUs only. A PMU's sampling rate is high (30 samples/second) and this research utilizes this high sampling rate in order to determine the security/insecurity of the operating conditions in real-time. Since the ML models have been trained on a 30 sample/second interval, a window of 30 samples is selected by the proposed DSA scheme

to ascertain the security of a system. Thus, the operator can accurately determine the security of a system with 1-second worth of PMU data. Lastly, this data is set as input to the previously built ML models. The operator can decide to test on the optimum ML model based on the performance classifiers that have been decided in Stage 2 of the assessment scheme.

2.2 Optimal PMU Placement

The objective of the PMU placement problem is to guarantee observability of the system with a required minimum number of PMU installations in the system model. There have been multiple PMU placement techniques such as the ones proposed in [46]-[48]. An integer programming based method is formulated as (2.1)-(2.2) to solve the above mentioned PMU placement problem [49].

$$min. \sum_{i=1}^{n} c_i . y_i \tag{2.1}$$

$$s.t\ f(Y) \geq \hat{a} \tag{2.2}$$

Where,

c_i is the cost of the placement of a PMU at bus i.

$\hat{a}$ is the $n * 1$ vector having all ones as it's entries.

Y is the vector which is binary indicating placement of a PMU.

The entries of the binary vector Y have been defined as follows:

$$y_i = \begin{cases} 1, & if\ a\ PMU\ has\ been\ installed\ at\ bus\ 1 \\ 0, & otherwise \end{cases} \tag{2.3}$$

The binary incidence matrix M is used to represent the system connection configuration having entries as follows:

$$M_{i,j} = \begin{cases} 1, & if\ i\ and\ j\ are\ connected\ or\ i = j \\ 0, & otherwise \end{cases} \tag{2.4}$$

To guarantee full observability of the system, each bus should have a PMU at the bus or should be connected via a transformer or a line to a subsequent bus which has a PMU installed on it. A $f(Y)$ matrix is thus constructed which will indicate the relevant connections between each bus and the PMU. If two buses are connected then the corresponding entry in the matrix would be a one otherwise it would be zero. The formulation of $f(Y)$ is given below, which is the product of the binary incidence matrix M and binary PMU placement matrix Y:

$$f(Y) = MY \tag{2.5}$$

The process for constructing the $f(Y)$ matrix for the IEEE 9-bus system is illustrated below.

The M matrix for the 9-bus system is given in (2.6).

$$M = \begin{bmatrix} 1 & 0 & 0 & 1 & 0 & 0 & 0 & 0 & 0 \\ 0 & 1 & 0 & 0 & 0 & 0 & 1 & 0 & 0 \\ 0 & 0 & 1 & 0 & 0 & 0 & 0 & 0 & 1 \\ 1 & 0 & 0 & 1 & 1 & 1 & 0 & 0 & 0 \\ 0 & 0 & 0 & 1 & 1 & 0 & 1 & 0 & 0 \\ 0 & 0 & 0 & 1 & 0 & 1 & 0 & 0 & 1 \\ 0 & 1 & 0 & 0 & 1 & 0 & 1 & 1 & 0 \\ 0 & 0 & 0 & 0 & 0 & 0 & 1 & 1 & 1 \\ 0 & 0 & 1 & 0 & 0 & 1 & 0 & 1 & 1 \end{bmatrix} \tag{2.6}$$

The IEEE 9-bus test system is shown below.

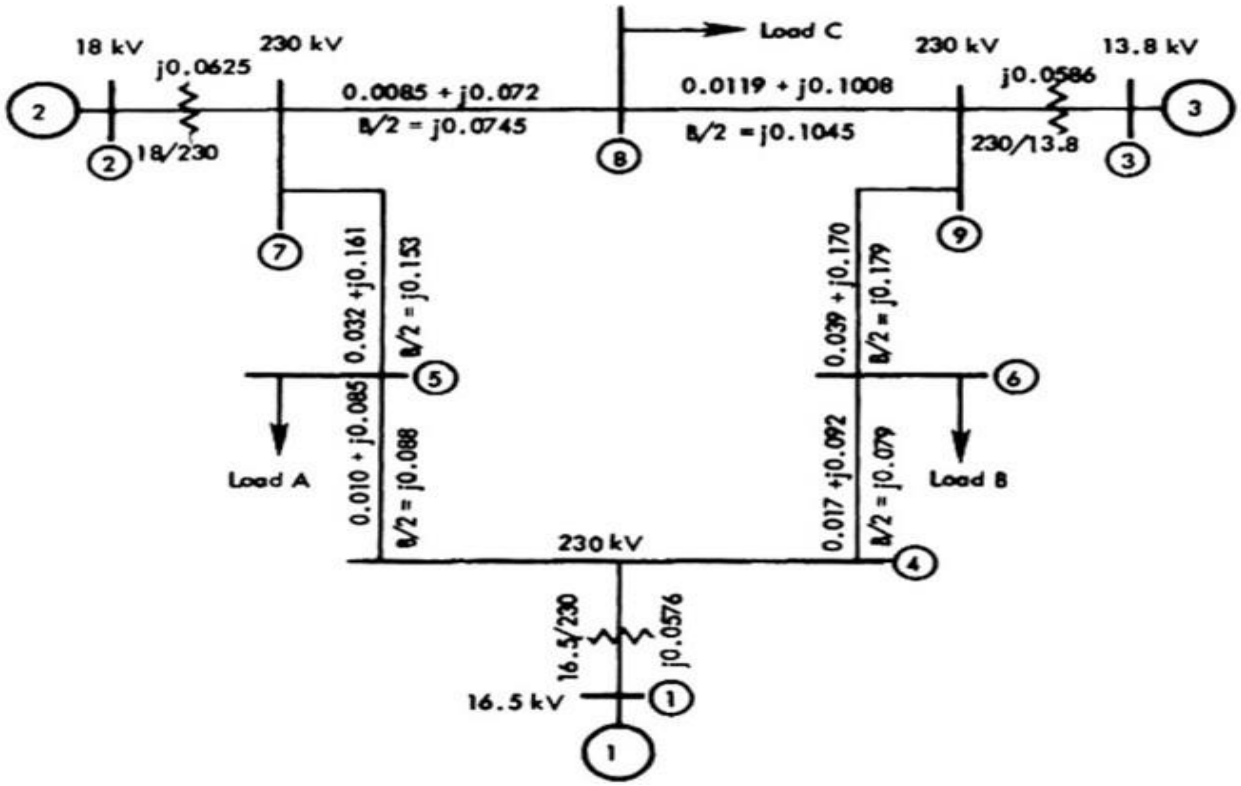

Figure 2. 2 IEEE 9 bus test system [50]

The inequality constraint for this system are:

$$f(Y) = \begin{cases} y_1 + y_4\ , & \geq 1 \\ y_2 + y_7\ , & \geq 1 \\ y_3 + y_9\ , & \geq 1 \\ y_1 + y_4 + y_5 + y_6\ , & \geq 1 \\ y_4 + y_5 + y_7\ , & \geq 1 \\ y_4 + y_6 + y_9\ , & \geq 1 \\ y_2 + y_5 + y_7 + y_8\ , & \geq 1 \\ y_7 + y_8 + y_9\ , & \geq 1 \\ y_3 + y_6 + y_8 + y_9\ , & \geq 1 \end{cases} \tag{2.7}$$

By taking the constraint at bus 2 as an illustrative example, we get $y_2 + y_7 \geq 1$. This indicates that at least one PMU should be installed at bus 2 or bus 7 to guarantee system observability for bus 2. Optimization results yield that PMUs should be installed at buses 4, 7, and 9 for the IEEE

9 bus test system to become completely observable by PMUs.

2.3 Comparison of the Transient Stability Assessment Methods

Machine Learning Algorithms have been used in this study to assess the transient stability required to implement a successful DSA scheme. In this study a synthetic database has been generated which replicates the huge amount of data that is generated by PMUs. A summary of the advantages and disadvantages of the five transient stability assessment methods introduced in Chapter 1 are summarized below in Table 2.1 [51]. ML algorithms can provide fast prediction results with considerable amount of accuracy with the support of a large database and real-time PMU-data.

2.4 Transient Stability Security Criterion

Transient stability is the ability of the power system to withstand severe disturbances, such as a fault on a transmission line. During a disturbance, a low frequency oscillation of generator angle δ will be superimposed on the synchronous speed ω_0. In this study DSA Tool's software TSAT is used to calculate the power angle based stability margin/index [52]. The index is defined for each island in the system:

$$\gamma = \frac{360-\delta_{max}}{360+\delta_{max}} * 100 \qquad -100 < \gamma < 100 \tag{2.8}$$

Where δ_{max} is the maximum angle separation of any two generators in the island at the same time in the post-fault response. The transient stability index for the system is taken as the smallest index among all islands. Thus, $\gamma > 0$ and $\gamma \leq 0$ correspond to stable and unstable conditions. Figure 2.3 illustrates the definition of this index. Angle margin (AM) is directly proportional to system angle separation and hence it gives a good indication of how severe a system is after a contingency. Table 2.2 depicts the relationship between δ_{max} and γ.

Table 2. 1 Comparison of the Transient Stability Analysis Methods [51]

Method	**Advantages**	**Disadvantages**	**Availability of pre-fault on-line DSA?**
Data Mining methods	Fast with reliable accuracy	Need a large database of data with online real time PMU measurements	Yes, available
Time-Domain Simulation	Accurate	Computational Burden	Yes, available
Probabilistic Methods	Takes consideration of risk probability	Heavy Computational Burden	Only for long term system planning
Dynamic State Estimation	Accurate	Need real time PMU-data	For post-fault online DSA
Energy Function Methods	Fast	Only for fast swing transient instability	Yes, available

2.5 Short Term Voltage Security Criterion

A system is considered to suffer from short-term voltage insecurity if the duration of any bus voltage remaining outside the range of 0.8 p.u. and 1.1 p.u. is more than 0.5 seconds [53]. The system is considered to be secure if the magnitude of the bus voltage recovers within that specified time frame even if the voltage dip or swell was previously more than 1.1 p.u. or less than 0.8 p.u.

Based on the criteria specified in Section 2.4 and 2.5, the system is considered to be insecure if any of the two criteria are violated during the time domain simulation conducted in this study. Transient stability criterion is first checked and then a check of voltage security is performed to determine the security or insecurity of operating conditions in the simulations performed. For generating the database of cases considered in this study, the secure operating points are labeled as 1 and the insecure operating points are labeled as 0.

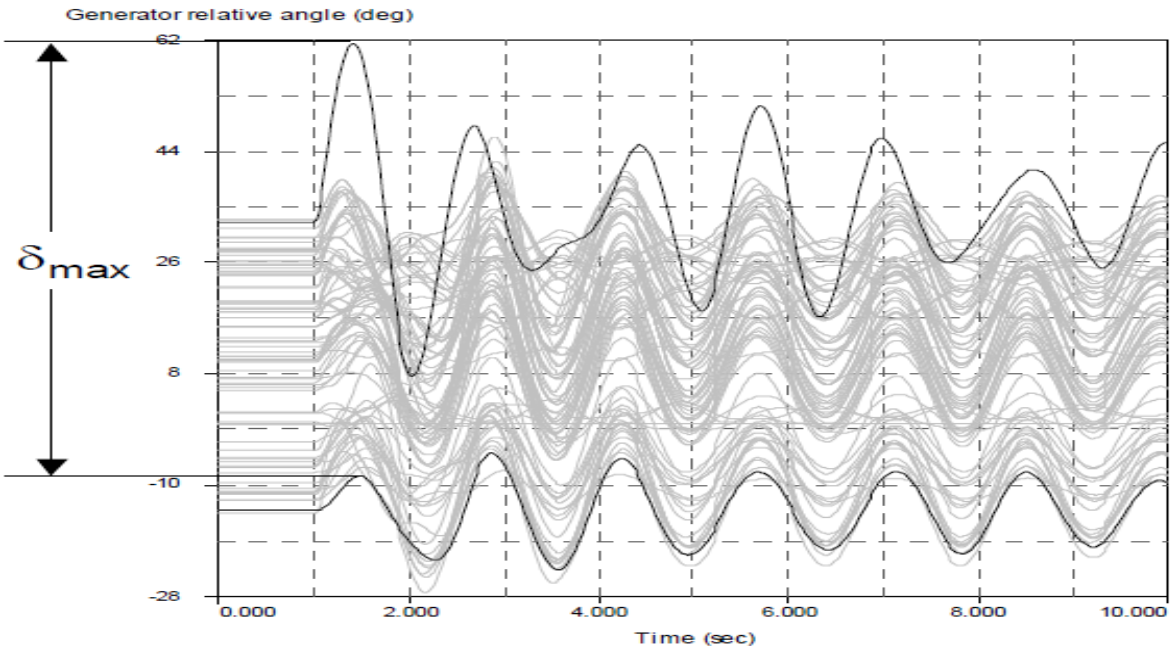

Figure 2. 3 Illustration of Angle Margin [52]

Table 2. 2 Relationship between $\delta_{max}$and γ

δ_{max}(degrees)	γ (%)
90	60.00
120	50.00
180	33.33
360	0.00

CHAPTER 3

3. OVERVIEW OF MACHINE LEARNING ALGORITHMS

3.1. Introduction to the Machine Learning (ML) Algorithms

In this study different ML algorithms have been employed to classify the security or insecurity of the operating conditions of the power system. Classification using a trained learning algorithm is the core of the task and every algorithm is a supervised learning method. Supervised learning is a technique, where a learning method is trained based on input datasets and associated responses, and at the end of the process, a function that would best describe the input datasets is obtained. In the proposed study, the datasets are operating conditions and contingencies, and the responses are the system security levels under the given operating conditions and contingencies. The different supervised learning algorithms that have been employed for the classification problem in this study are Decision Tree (DT), Random Forest (RF), Support Vector Machine (SVM), and Multi-Layer Neural Network (MLNN).

3.1.1 Decision Tree (DT)

Decision Tree has been on the most popular classification algorithms used for Transient Stability Assessment as a part of a DSA scheme and has been significantly used in [54][55]. In [55], the authors used both the classification as well as the regression tree for determining voltage stability prediction as well as transient stability. DT have been used to analyze synchrophasor data in [56], [57] .DT is essentially a supervised learning technique which is used to determine prevalent relationship scenarios in the provided data-set and subsequently classify the given data based on partitioning with the help of if-else statements. In this study, a classification and regression tree (CART) based DT has been trained offline with the help of a training database and a model has

been developed by forming correlations between the input and the output. In Fig. 3.1, a DT structure example is presented where the parent node represents the entire data set. The process of splitting is continued at each node till no further splits are possible.

After obtaining the trained DT, testing data set values are fed into the built model process through if-else statements and subsequently a decision is obtained which is usually based on splits on each node which are predetermined. Terminologies with respect to DT are given below in [58]:

- *Size:* The total size of a given DT is given by the total number of nodes present in the entire tree.
- *Depth:* The depth of a given DT is the longest path traversed between the parent node and the leaf node. In Fig. 3.1, the root is the parent node and the while the splitting nodes are given by the leaf nodes. The depth of this tree is 4.
- *Pruning:* Pruning is defined as the process with the help of which the size of the DT is greatly reduced by removing certain sections of the tree which are less significant than the others. Pruning affects the overall accuracy of the DT.

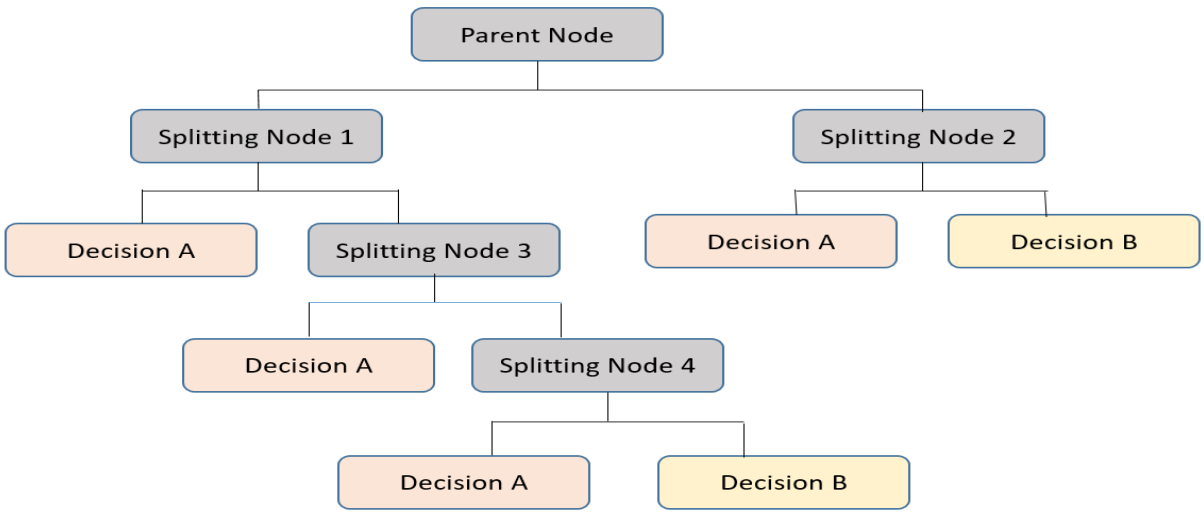

Figure 3. 1 CART Example

3.1.2 Random Forest (RF)

Random Forest is an ensemble learning technique of classification or regression that operates by constructing a multitude of decision trees during training phase and later outputs the class that is the mode of the classes (for a classification problem) or the mean prediction (for a regression problem) of the individual trees [59]. RF have been used in power system to correctly analyze voltage security in [61], fault detection in [62] and accurate PV power forecasting in [63]. The structure of RF is constructed of de-correlated DTs in which each node of the DT would depend on a vector which has been selected randomly from the entire length of predictor vectors. In order to create many datasets of the same size, *bootstrap sampling* method is employed by the RF which randomly samples the cases by replacing it from the existing database multiple number of times. This is done in order to have a better estimation of the given database which would subsequently enhance the accuracy of the predicted model. About one third of the cases are left out of the bootstrap sampling method while constructing each tree which is defined as the – Out of Bag Dataset – which is later on used for the testing model.

The procedure for creating an RF model is described below in Fig. 3.2 [64]. The final classification output (i.e., Secure or Insecure) of an RF model is the majority voting result (largest fraction) from a large number of DTs. Although each DT is unpruned and over-fitted, the overall RF model can benefit from aggregated base variance reduction model. Details of the RF algorithm has been presented in [65].

Let us assume we have a database of N number of cases. Each case is being represented by P number of predictor values with one target as the goal. The z^{th} case which currently contains the measurement of z number of cases, $y_z = \{A_1, A_2, \dots, A_z\}(z = 1\ to\ N)$ with one target as the goal, $T_z = \{In\ or\ Se\}$, where secure is "Se" and insecure is "In" state All the cases which accounts for

the security or insecurity of the z number of cases are processed through time-domain simulations. If we have a RF model which contains D number of trees, the process of training is that for each of the nodes in the d^{th} tree where $d \leq D$, the vectors which are a subset of the original vector set $\emptyset_m$ is to be selected from P predictor values . The d^{th} tree is constructed by using the training database F_d from the d^{th} bootstrap sampling and $\emptyset_d = \{\emptyset_1, \emptyset_2.., \emptyset_{m-1}\}$ which would make the number of classifiers as $G_d(F_d, \emptyset_d)$. Thus, the RF model is composed of a collection of D number of tree which are structured classifiers J_{RF}^d as defined in (3.1).A voting scheme is established to find the tree which would lead to the construction of the optimal forest .A majority voting scheme is thus employed to take into account each tree that has been constructed in the training phase. For all the DT that has been constructed in the training phase, each of them gives a predictor value at the terminal nodes which can be wither secure or insecure Each DT would ultimately give a vote for the class which would be the most popular for any input y_p for which a RF model would thus be constructed across all DT as shown in equation (3.2).

$$C_{DT}^k = \{T_k(X_k, \theta_k), k = 1,2, \dots, N_{tree}\} \tag{3.1}$$

$$C_{DT}^{N_{tree}}(x_i) = majority\ voting\{C_{DT}^k(x_i), k = 1,2, \dots, N_{tree}, x_i \in X\} \tag{3.2}$$

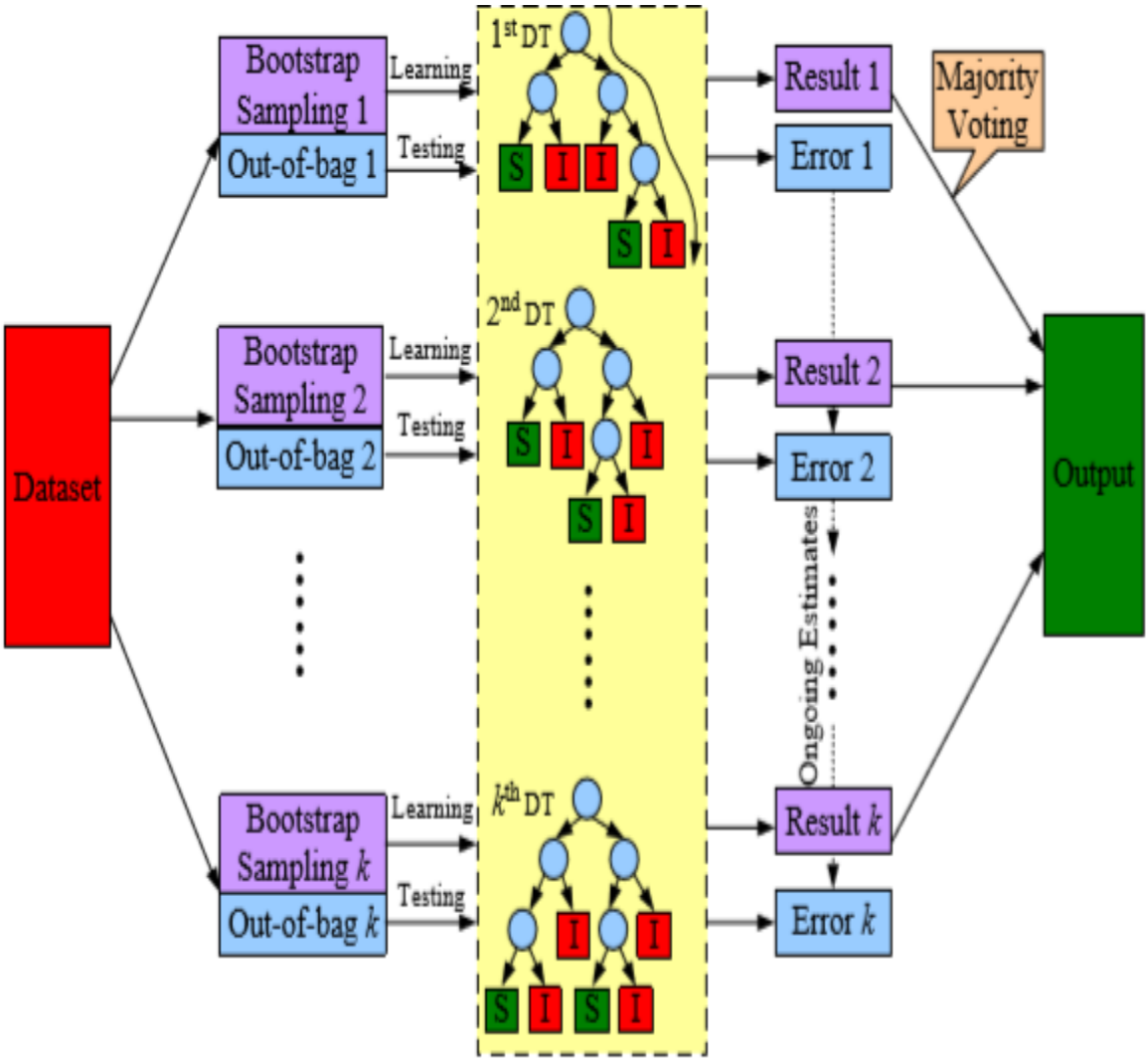

Figure 3. 2 Structure of a RF model [64]

3.1.3 Support Vector Machine (SVM)

SVMs are machine learning models which have been based on theoretical results from the statistical learning theory [66].SVMs have been used in power system to accurately determine risk assessment in [67], reliability evaluation in [68] , security alert system in [69] and method for voltage control have been proposed in [70]. An SVM classifier minimizes the generalization error by optimizing the tradeoff among the number of training errors and the Vapnik–Chervonenkis (VC) dimension. A theoretical bound exists for the generalization ability of the SVM which

depends on the number of training errors (t), the size of the training set (N), the VC dimension associated with the resulting classifier (h), and a confidence measure for the bound itself (η) [66].

$$R < \frac{t}{N} + \sqrt{\frac{h\left(ln\left(2N/h\right)+1\right)-ln\left(\eta/4\right)}{N}} \tag{3.3}$$

Eq. (3.3) gives the risk R which represents the classification error expectation over the entire population of input/output pairs.

SVM is a learning algorithm which classifies the samples using a subset of training samples called support vectors. The main idea behind a SVM classifier is the algorithm tries to create a feature space while using the given attributes found in the training database. Subsequently it tries to find a boundary or a limiting plane which would separate the feature space into two halves which would exactly contain the training points which would belong to the specific category. In this study the specific points would be secure and insecure points in the training database. This has been replicated in Fig. 3.4.

In Fig. 3.3, the star data points belong to one category of classes while the circular points is of the other category. SVM essentially tries to find a hyperplane (P_1 or P_2) which would optimally split the data points into two categories .There may be a multitude of hyperplanes that can be constructed, in the figure given below a linear hyperplane is considered. SVN tries to choose the best decision boundary which would segregate the data based on the "maximum margin hyperplane concept". Parallel supporting hyper planes are associated with each of the hyperplanes P_1 and P_2. In the figure described below, although each of the hyperplanes is able to divide the points into two categories the margin associated with P_1 is larger and hence P_1 is chosen as the optimal hyper plane .Thus the larger the margin ,lesser will be the generalization error.

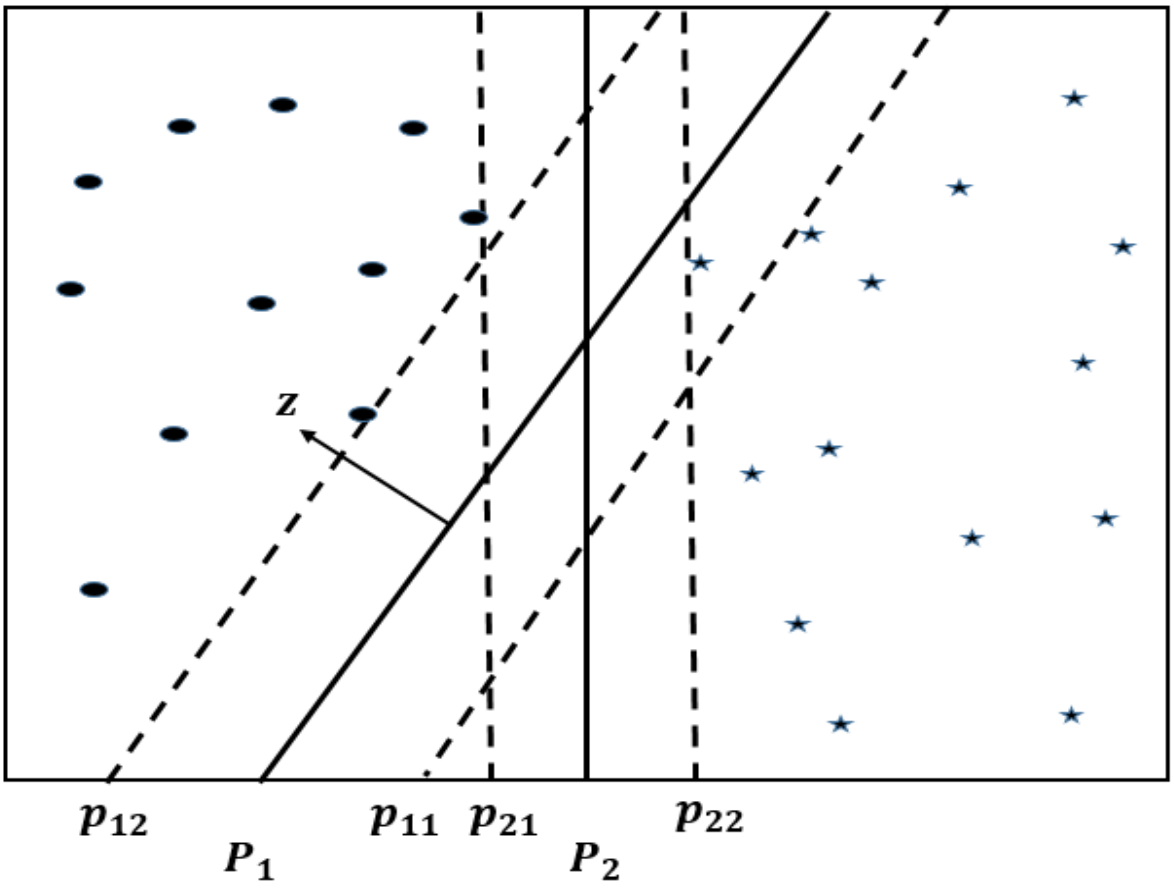

Figure 3. 3 Decision boundary and margin of SVM classifier

Two types of SVMs exist, (1) Linear SVM, which separates the data points using a linear decision boundary and (2) Nonlinear SVM, which separates the data nonlinearly. For a given linear SVM the equation for the decision plane is given by

$$z.y + g = 0 \tag{3.4}$$

Where z and y are the vectors and the direction of z is exactly perpendicular to the linear decision plane. Given any set of data points y_k the equation for the decision plane when the points lie above the plane is given by

$$z.y_k + g = z, \ \ where\ z > 0, \tag{3.5}$$

When the points lie below the decision plane, the equation is thus given by

$$z.y_k + g = z, \ \ where\ k < 0, \tag{3.6}$$

The distance between two planes is constructed as the margin a which is shown below:

$$d = \frac{2}{||z||} \tag{3.7}$$

The main aim of SVM classifier is to maximize the value associated with a. This is equivalent to minimizing the value of ${||z||^2}/{2}$ .The corresponding values of z and g are guaranteed by solving a set of quadratic equations under the following constraints:

$$z.y_k + g \geq 1, \ \ if\ m_k = 1, \tag{3.8}$$

$$z.y_k + g \leq -1, if\ \ m_k = -1, \tag{3.9}$$

Where, m_k is the class variable associated with y_k. The optimization problem is thereby solved by using Lagrange multiplier method. The objective function which needs to be minimized in the Lagrangian form is thereby constructed as follows:

$$Z_o = \frac{1}{2}||\mathrm{z}||^2 - \sum_{k=1}^{M} \rho_k (m_k(z.y_k + g) - 1) \tag{3.10}$$

Where, ρ_k are Lagrange multipliers and M are the total number of samples in the data.

Nonlinear SVM classifier tries to transform the dataset into a higher dimensional space where the data itself can be exactly separated using a linear decision plane. This however increases the complexity of the classifier.Mapping function while transforming the data space is also unknown. These shortcomings can be overcome by using a concept called the *kernel trick* which would essentially shift the available data to a higher dimensional space. If we are given δ as the mapping function, a nonlinear decision plane can be transformed into a set of linear planar equation as follows:

$$z.\delta(y) + g = 0 \tag{3.11}$$

The parameters which need to be tuned in an SVM classifier are penalty C and gamma γ . C is a regularization parameter which controls the tradeoff between achieving a low error on the training data and minimizing the norm of the weights. It essentially forces the SVM optimization to avoid

any misclassification in the training example. The higher the value of "C", the more the penalty, leading the classification model to over-fit the data. Conversely, smaller value of "C" leads to a more generalized model which will not be able to classify the unknown data accurately. The parameter γ is defined as the inverse of the radius of the influence of samples selected by the model as support vectors. The behavior of the model is sensitive to the γ parameter which indicates that if the value of γ is too large, the radius of the area of influence of the support vectors will only include the support vectors itself and it will lead to a problem of overfitting in the data. Conversely if the value of γ is too small, the model will be constrained and will not be able to capture the complexity or variations in the dataset. Radial-based function (RBF) kernel with grid searching was used in the SVM model and optimum values for the parameters of RBF (C and γ) were determined.

3.1.4 Multi-Layer Neural Network (MLNN)

Artificial Neural Network (ANN) can be defined as a highly connected array of elementary processors called neurons. ANN have been widely used in the power system domain for adaptive control of stabilizers in [71], assessing transient stability in [72],determining security of power plants in [73].They are electronic networks based on the neural structure of the brain. Neural networks are typically organized in three distinct layers viz. input layer, hidden layer, and output layer. These layers are connected with the help of a number of nodes which contains an activation function in the hidden layers. The input to the network are different patterns of the input data, subsequently the input later is connected to the hidden layer where it is processed by weighted conditions. After the processing and readjusting of the weights, the weighted conditions are processed between the hidden layer and the output layer. After this step the output layer is obtained. The simplest architecture of a neural network has been shown in Fig. 3.4.

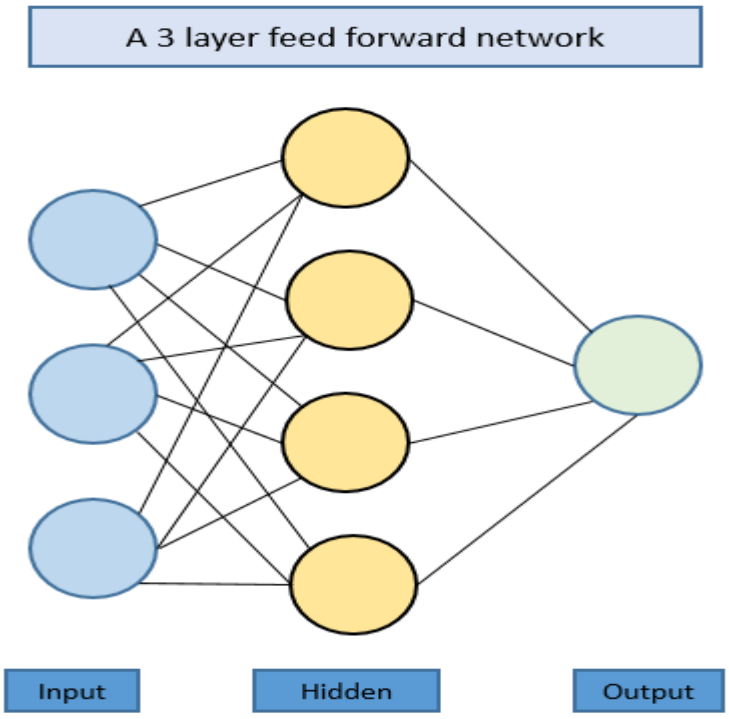

Figure 3. 4 Neural Network Model

In this study a feed forward neural network called a multilayer perceptron (MLP) will be employed [74]. Fig. 3.5 gives the behavior of a single artificial neuron. An artificial neuron takes in a set of weighted inputs and applies an activation function to their sum. In Fig. 3.6, y referes to an input, x is the weight, and g is the bias term.

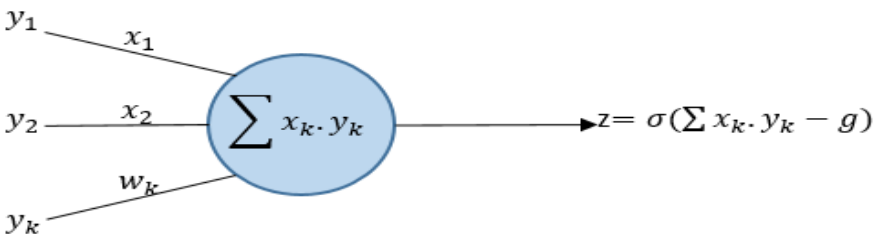

Figure 3. 5 Artificial Neuron Diagram

A neural network with k input nodes and 1 output node serves as a function with k inputs and 1

output. The goal in this study is to use a set of k-dimensional training patterns with known ouptus which will be used to train the network such that the output is either a negative or positive output.Subsequently the network is used to classify the unknown patterns. A feed-forward network such as MLP with a single hidden layer is capable of giving a deisred accuracy for classification upto certain limits . Lack of desired accuracy and success of the network can be either dure to lack of adequate number of training inputs,highly inusfficient number of hidden layers,lack of a better ativation function for the designed network,failure of a constrained relationship between the ouptut and the input layers [75].

Training of a neural network involves solving a nonlinear optimization problem where the goal is to minimize an error function depending on the type of network chosen. Different gradient techniques are available online which are chosen during the training phase to reduce the problems that arise due to prsence of local minima. In this study, the gradient descent method [76] has been used in order to solve the optimization problem.

By using a basic logistic activation function ,a basic three layer feed forward network is hereby explained. If a pattern is taken with p inputs and the number of nodes in the hidden layer is assumed to be z, the input to the j^{th} node is as follows:

$$\sum_{k=1}^{p} x_{kj} y_k + g \tag{3.12}$$

Where, y_k is the k^{th} input and weight is given by x_{kj} between the k^{th} input node and j^{th} hidden node. Thus the output from the j^{th} hidden node is as follows:

$$l_j = \sigma(\sum_{k=1}^{p} x_{kj} y_k + g) \tag{3.13}$$

Where the considered $\sigma(y)$ is the activation function.

The output obtained from a network is given by the following equation:

$$\sum_{j=1}^{n} \gamma_j l_j \tag{3.14}$$

Where, l_j is the output from the j^{th} hidden node and γ_j is the weight from the j^{th} hidden node to the ouput node. The output is given as:

$$z = \sigma(\sum_{j=1}^{n} \gamma_j \sigma\,(\sum_{k=1}^{p} x_{kj} y_k + g)) \tag{3.15}$$

The method for updating the input weights is known as back propagation. For a given set of p-dimensional inputs ,the goal is to minimize the error between the neural network output and the target value. The error is thus given by a function of weights which is as follows:

$$E(g_1, g_2, g_3, \ldots, g_n, \gamma) = \frac{1}{2}(z - m)^2 \tag{3.16}$$

Where, g_n is the p-dimensional vector of weights between the inputs and the n^{th} hidden node and γ is the vector of weights between the hidden nodes .The ouput value is thus given by z.

In the proposed study, a self exponential linear unit (SELU) has been used [77] as the activation function. SELU has self-normalizing properties because the activations that are close to zero mean and unit variance, when propagated through many network layers, will converge towards zero mean and unit variance. This, in particular, makes the learning highly robust and allows to train networks that have many layers or in other words it is practical to use SELU in case of deep learning networks. The number of hidden layers is also set to 5 which makes it a Multi Layer Neural Network with different number of neurons in each of the hidden layers.

3.2 Input Parameters to the ML Algorithms

Since the above mentioned algorithms are supervised learning techniques, the training dataset contains the labeled parameter of the bus voltage magnitudes and bus voltage angles obtained from PMUs. The labels associated with each of the training samples are binary, i.e. either it is 1 which specifies that the condition is secure or 0 which specifies that the working condition is insecure. This classification is based on extensive time-domain simulations perfomed offline while generating the database of cases. During the testing phase of the algorithms the labels are removed

and the bus voltage magnitudes and bus voltage angles along with the PMU errors are fed into the trained ML models to accurately classify the security/insecurity of the operating conditions.

CHAPTER 4

4. CASE STUDY: IEEE 118 BUS SYSTEM

4.1 IEEE-118 Bus Test System

To verify the performance of the proposed DSA technique in Chapter 2.1, the simulations were carried out on the IEEE-118 bus system as shown in Fig. 4.1. The 118-bus system is a simplified model of the American Electric Power (AEP) system as of December 1962 [78]. The system consists of 118 buses, 54 generators, 177 transmission lines, and 9 transformers.

4.2 Incorporation of Seasonal Load

In the literature survey conducted for this study, it has been found that previous works have often built their DSA scheme based on a single normative day for the entire year. Since loads vary significantly with different seasons, it makes sense to replace the single normative day load profile by load *profiles* that depict accurately the load change occurring in different seasons. Therefore, in this study, an attempt has been made to segregate the year into 4 seasons, namely, spring, summer, fall, and winter to create four normative load profiles that can more accurately represent the load variations for different seasons. Each season roughly comprises of 90 days and an aggregate of the daily load profile for these 90 days has been made and combined to create a single normative day, which best represents a given season. In [79], CAISO has uploaded the hourly load profile for its energy management system (EMS) for the years 2014-2017. Utilities that have provided their data making up the daily CAISO load include Pacific Gas and Electric (PG&E), San Diego Gas and Electric (SDG&E), Valley Electric Association (VEA), and Southern California Edison (SCE). In the uploaded database, EMS hourly load for the entire year is present. Based on the duration of the four seasons, namely, spring (March to May), summer (June to

August), fall (September to November), and winter (December to February), four normative load profiles have been created.

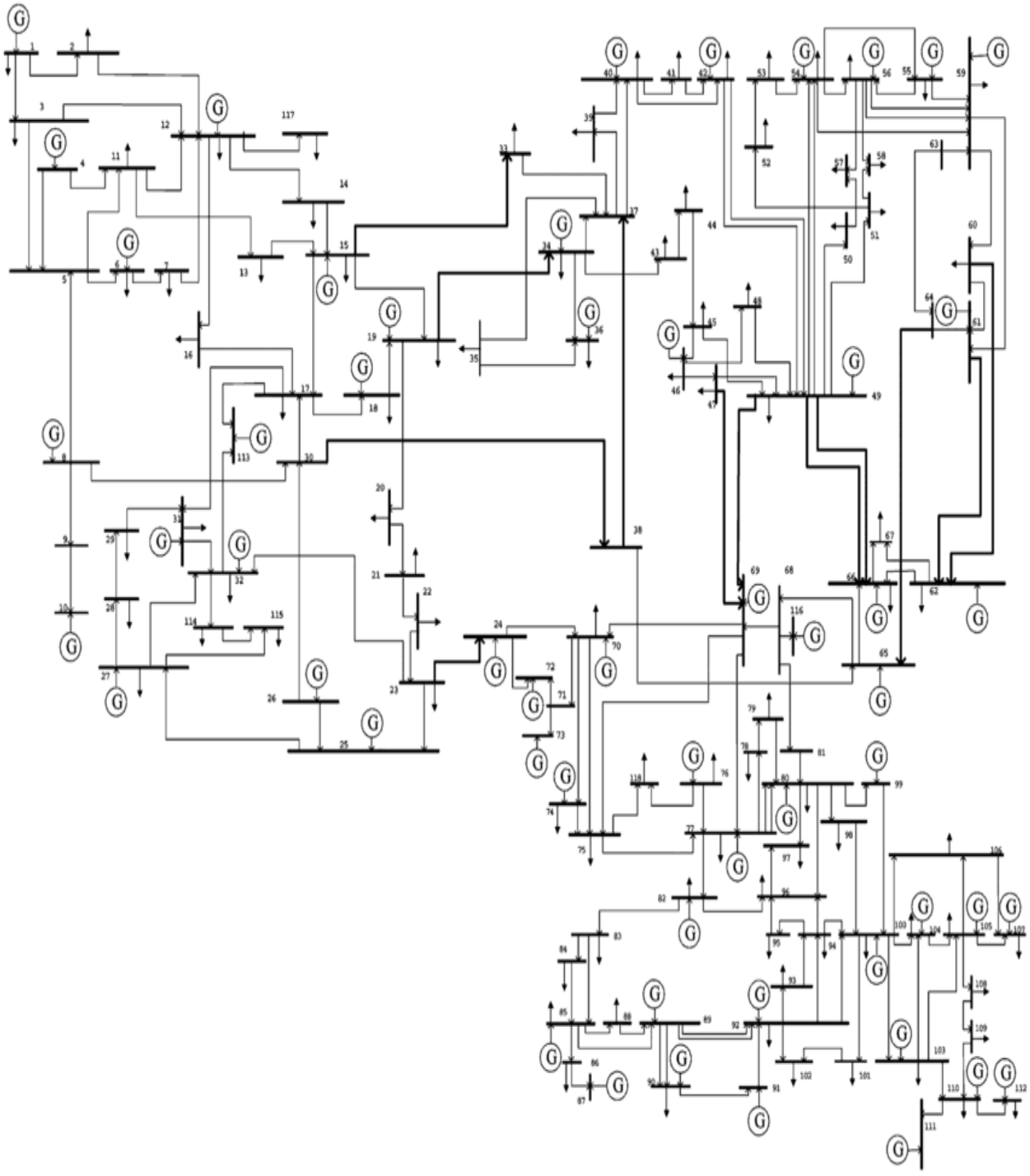

Figure 4. 1 IEEE-118 Bus System

Based on the hourly load for each of the 90 days for a season, an average has been taken for each of the 24 hours to find the net load curve that would represent a single day, which would best represent each season. The process is repeated for 4 years' worth of data to take into account any load change that might have happened over the years. The normative load profiles have been shown below in Figs. 4.2, 4.3, 4.4, and 4.5

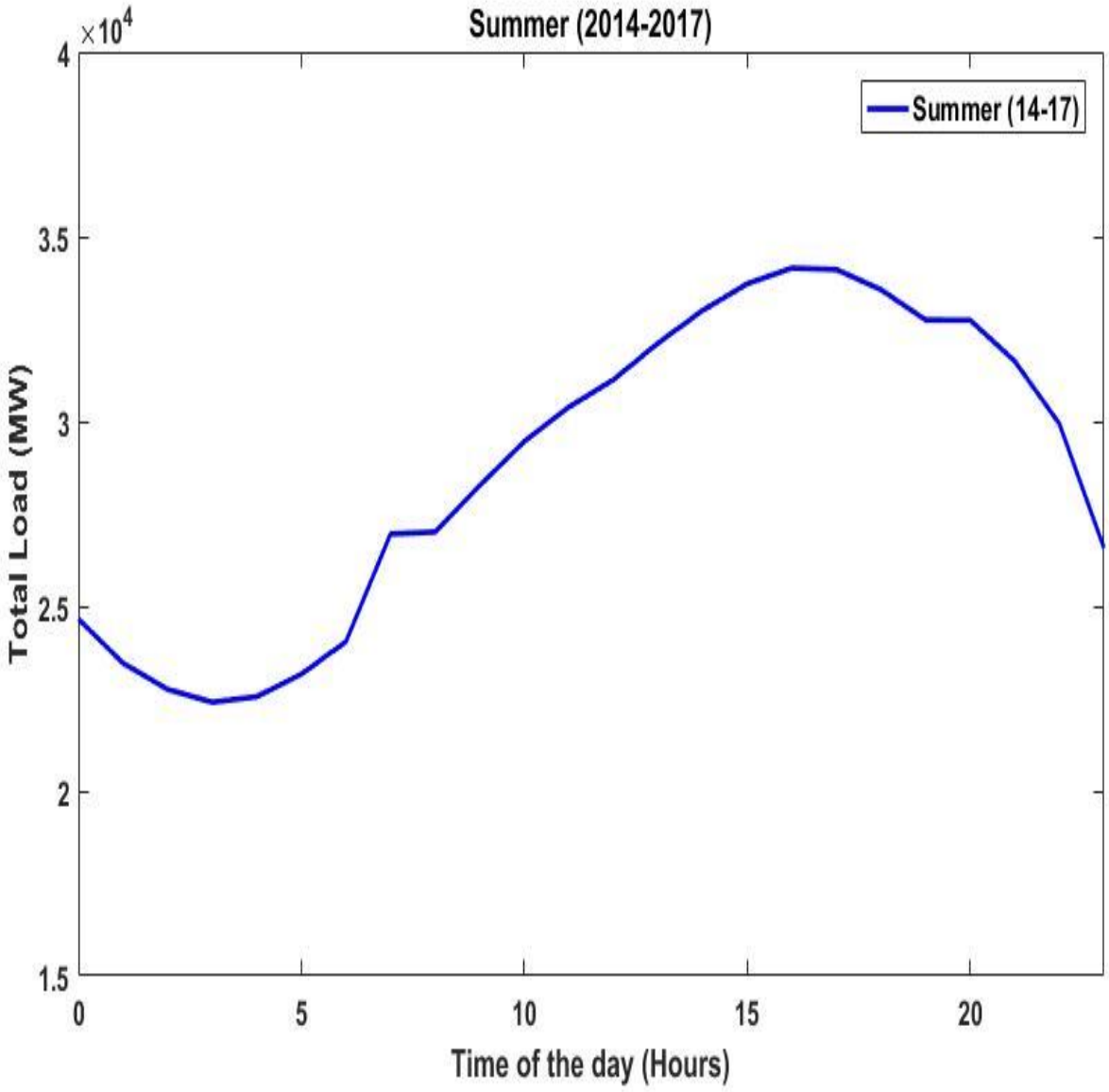

Figure 4. 2 Summer Daily Load in MW

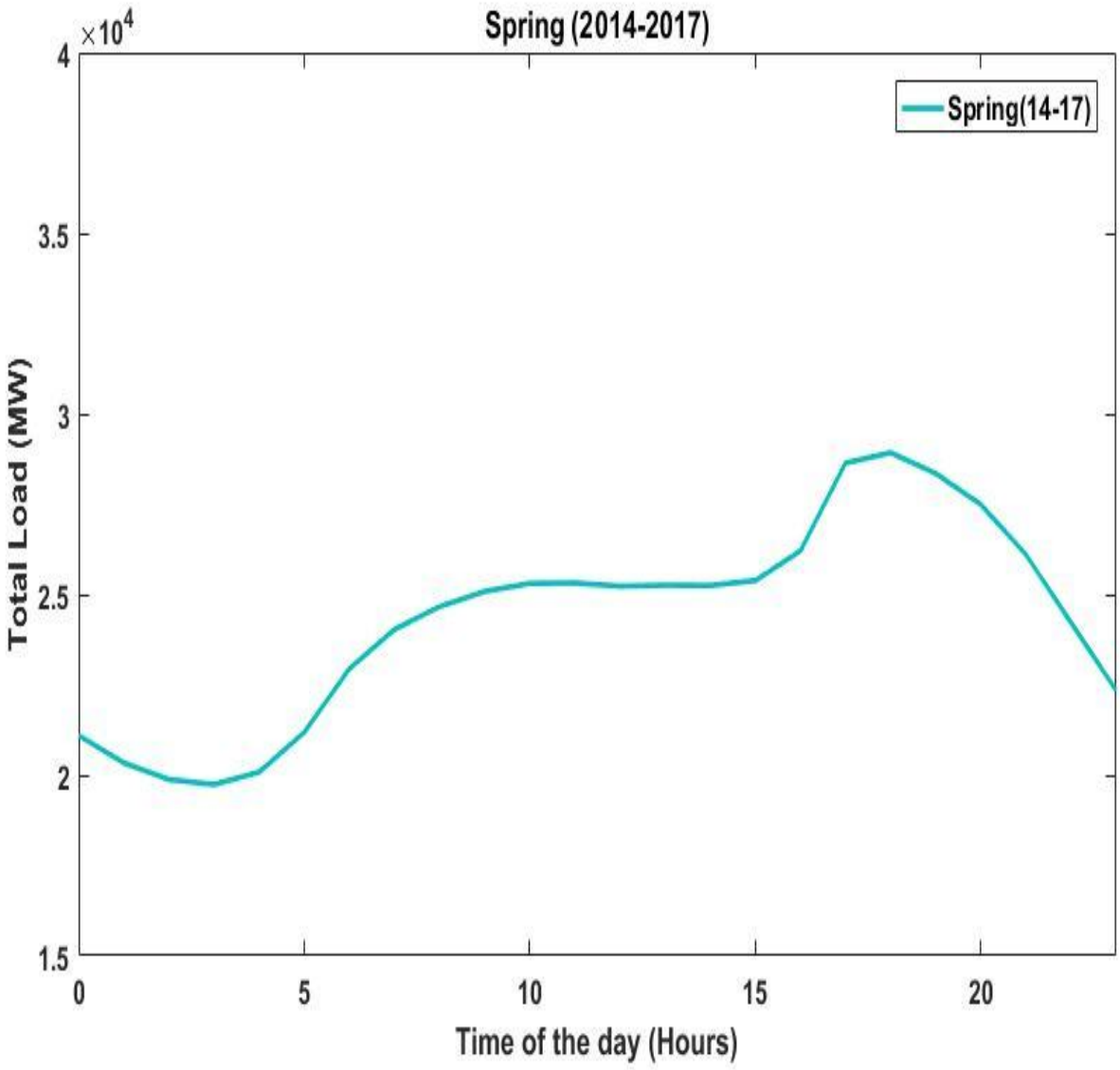

Figure 4. 3 Spring Daily Load in MW

Load changes that might have occurred during 4 years' time have been averaged out to better account for system change that might have happened. An average has been taken as it is the simplest way to represent the growing load trend provided in the historical hourly EMS load database provided by CAISO.

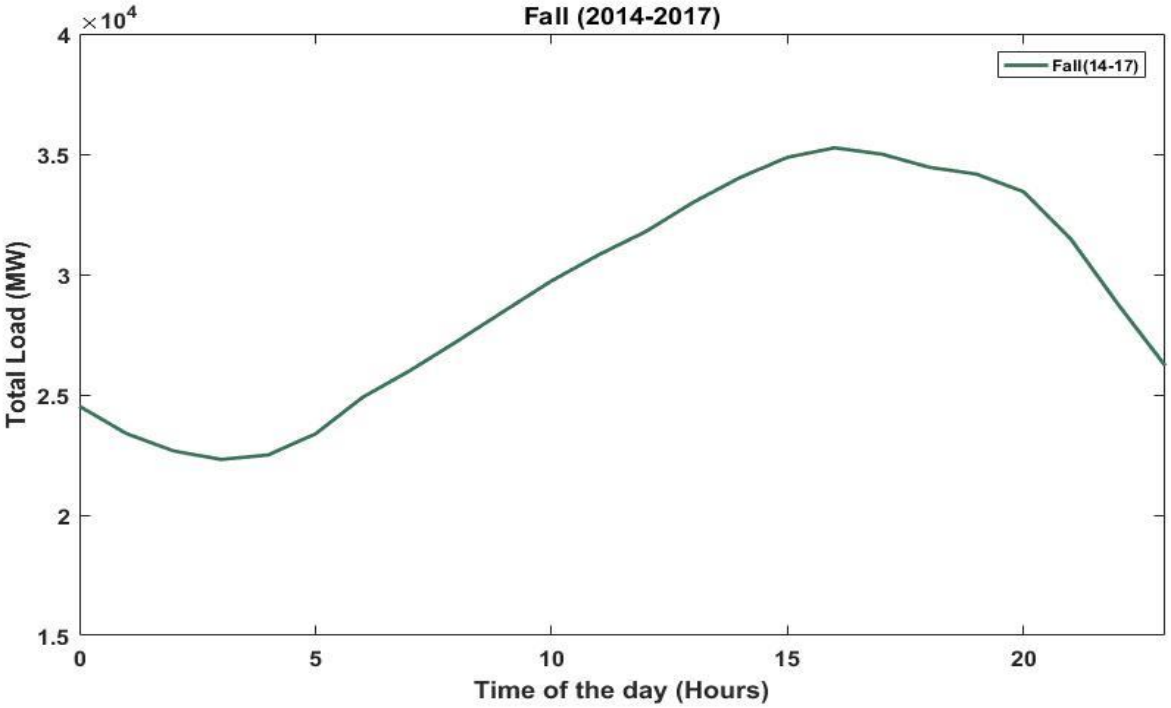

Figure 4. 4 Fall Daily Load in MW

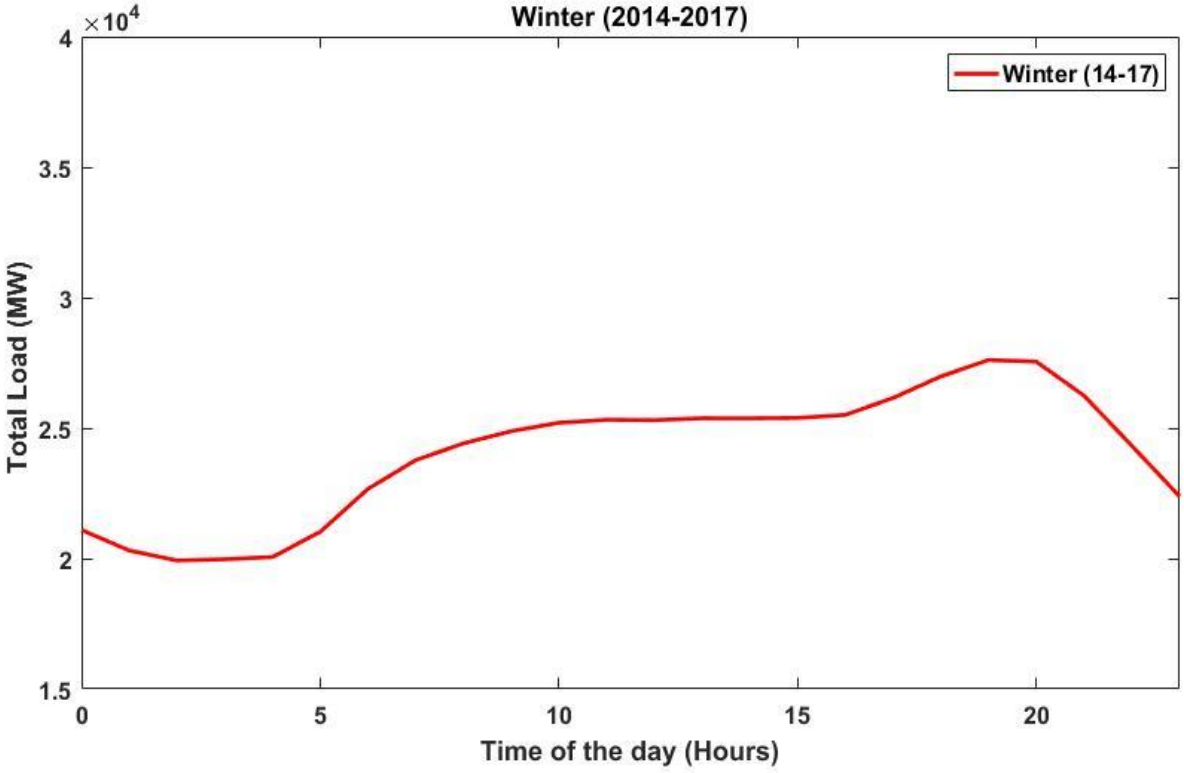

Figure 4. 5 Winter Daily Load in MW

Based on the above four figures of load profiles, each normative day is split into 15 min intervals in order to generate 96 Operating Conditions (N_{oc}) for a single day. Industrial standards [80] state that optimal power flow (OPF) must be performed at least every 15 minutes in order to account for better system security of the interconnected network. Hence, a 15-minute interval has been chosen as a part of this study for generating the operating conditions. Based on 96 N_{oc} for a single day, multiple contingencies have been run to generate the database of cases that has been discussed in subsequent sections. Thus, in order to account for four different days of the year, learning algorithms have been trained and tested separately for each season to accurately represent the variations in load that occurs with the change in seasons.

4.3 Solar Modeling

Power systems all over the world are seeing increased penetration of renewable energy sources, which are replacing conventional plants driven by fossil fuel. According to Western Electricity Coordinating Council (WECC), the total generation of solar and wind in 2015 in the Western Interconnection is approximately 7% [81]. Solar energy has been touted as one of the primary sources of clean energy since the past decade. To account for different levels of solar penetration in the system, a net solar generation curve has been selected from the CAISO website [82]. This is depicted in Fig. 4.6. Based on the net solar generation curve, as shown in Fig. 4.6, the total amount of solar penetration considered for this study on the IEEE-118 bus system is 10% and 20%, respectively, of the total generation. The 118-bus system has a total real power generation of 3,793 MW and electrical load of 3,668 MW, respectively. Therefore 10% of the entire generation is approximately 379.3 MW and 20% of the total generation is 758.6 MW. Accordingly, several conventional generators in the 118-bus system have been replaced with solar

PV to account for 10% and 20% of solar generation. In order to account for varying solar output throughout the day, the total solar generation has been replaced with varying *generation factors*. That is, the peak solar generation which occurs at 12:15 pm of the day accounts for generation factor of 1 and correspondingly all the other times of the day have a solar generation factor of less than 1. For example, at 2 PM the solar generation factor is 0.9. Thus at 2 PM, the solar generation for 10% penetration for the IEEE 118-bus system would be $0.9 * 397.3\ \text{MW} = 357.57\ \text{MW}$ and for 20% penetration, the total solar generation in the IEEE 118-bus system would be $0.9 * 758.6\ \text{MW} = 682.74\ \text{MW}$.

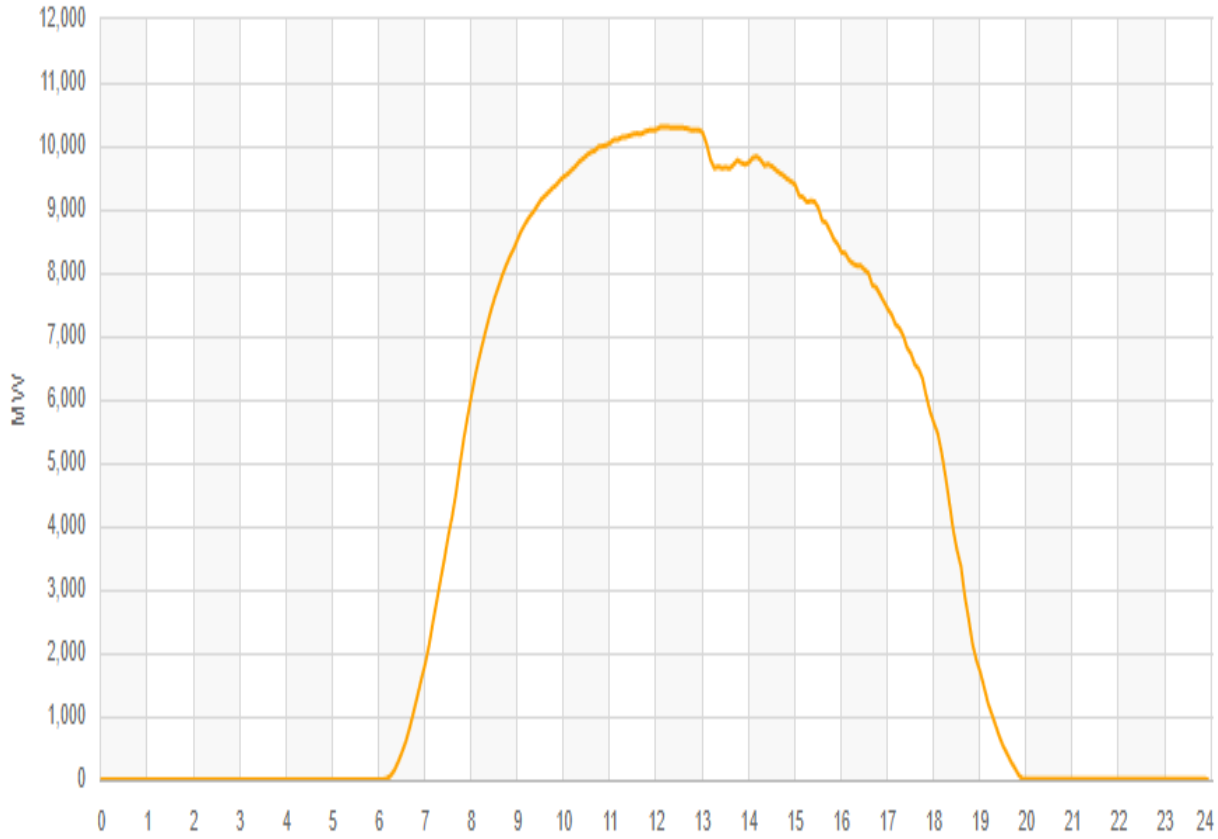

Figure 4. 6 Solar Generation in Megawatts for a 24 hour period

4.4 Solar Energy Integration

Solar cells also called photovoltaic (PV) cells convert sunlight directly into electricity. PV gets its name from the process of converting light (photons) to electricity (voltage), which is termed as the PV effect [83]. Most PV systems are of three types, namely, residential scale (up to several kW), commercial scale (up to several MW) which are connected to distribution feeders, and large generation facilities (which might exceed 100s of MW) and are connected to the transmission system.

Solar power plants are different from conventional power plants. Their interface to the grid is an inverter connected to a PV array. The inverters are characterized by low short circuit current, lack of mechanical inertia, and fast controls. The main function of the inverter control is to make efficient use of the energy being produced by the PV array while maintaining the magnitude of AC current such that the ratings of the inverter is not exceeded.

In accordance with the WECC PV Plant Power Flow Modeling guide [84], PV plants must be represented by a system consisting of one or more equivalent generators and unit transformers, equivalent collector system, substation transformer, and plant level reactive support system as shown in Fig. 4.7 [85].

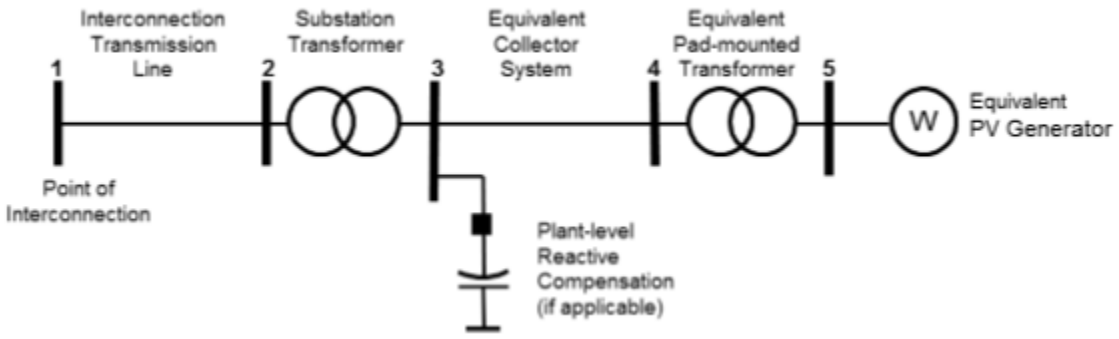

Figure 4. 7 PV Power plant [85]

Dynamic representation of large-scale PV-plants requires the use of the renewable energy modules. GE PSLF software is used to create the dynamic representation of these models which are then exported to TSAT software to carry out the simulation studies. The modules that were used in this study are:

- REGC_A module: This is used to represent the Generator/Converter (inverter) interface with the grid. The module processes the real and reactive current command and also the real and reactive current injections which are fed into the grid.
- REEC_B module: This is used to represent the electrical controls of the inverters. The module provides real and reactive current commands to the REGC_A module.

4.5 Database of Cases

The training process of the machine learning (ML) algorithms that have been employed in this study must be based on a database of cases that are generated offline through exhaustive time-domain simulations. For a normative daily load profile corresponding to different seasons, 96 N_{OC} have been selected. An exhaustive scheme has been employed to generate contingency cases N_C based on opening of lines due to three-phase faults. Specific security criteria that deal with voltage and frequency stability are then checked to determine the security classification for each case. The classification is always binary, i.e. “insecure” (if bus voltage violation has occurred) or “secure” (if no bus voltage violation has occurred).

After the binary classification is specified, the database of $N_C * N_{OC}$ is split into training and testing phases, which is then fed into the different ML modules. The training percentage is kept at 70% of the total dataset while the remaining 30% of the data is used for testing. Additionally, 10% of the training data is used for validation of the different learning algorithms. Based on the value of

power that the lines are carrying in the 118-bus system, a list containing 50 contingencies is prepared. Thus, for a single day, the total number of cases that have been generated is $96 * 50 = 4800$. Multiple '$N-1$' and '$N-k$' contingencies have been selected to represent secure as well as insecure states of the system. For generation of scenarios, a three-phase line to ground fault has been initiated at 10% of the length of the line and the fault has been cleared after 0.12 seconds. Subsequently, the line has been opened. This process has been also repeated for '$N-k$' contingencies where multiple faults occur in different lines at the same time. The time-domain simulation has been carried out on a desktop computer with Intel Core i7-6700 CPU @ 3.4 GHz with 16 GB RAM. The database not only contains the measurement data as predictor values, i.e. bus voltage magnitude and bus voltage angles obtained from the PMUs placed in the system, but also the target values which are the result of time domain simulation, namely, secure (1) or insecure (0), based on the criteria given below:

- Transient Stability: The system is considered as transient unstable for a given contingency if the system's transient stability index (TSI) defined by (4.1) is lower than 10% in which $\Delta\delta_{max}$ is the maximum angle separation of any two rotor angles in degrees. The TSI in (4.1) is based on TSAT's power swing-based algorithm [52].

$$TSI = \frac{360-\Delta\delta_{max}}{360+\Delta\delta_{max}} * 100\% \quad (4.1)$$

- Short-term Voltage Security: The system is considered to be insecure if the voltage of any bus voltage goes outside the range of 0.8 p.u. - 1.1 p.u. for longer than 5 seconds.

Thus, for each seasonal load profile as well as for varying levels of solar penetration 4,800 cases have been generated. Each individual simulation is run for 20 seconds where contingencies i.e. '$N-1$' or '$N-k$' have been initiated every 5 seconds. Since PMUs have been installed on the system, each second worth of data consists of 30 samples. Thus, for a time window of 20 seconds,

there are a total of 600 samples.

During the online security assessment step, measurements obtained from PMUs, i.e. bus voltage magnitudes as well as bus voltage angles, are cross-validated with the previously built ML model to classify the security or insecurity of the operating point in real-time.

4.6 Performance Criteria for the Machine Learning Algorithms

In this analysis, different performance metrics for classification problems are used. From the classification matrix of a binary classifier, the following values are obtained, namely, True Positive (TP), False Negative (FN), False Positive (FP) and True Negative (TN). A brief overview of each of these terms is provided below.

	Predicted Class		
Actual Class		Class = Yes	Class = No
	Class = Yes	True Positive	False Negative
	Class = No	False Positive	True Negative

Figure 4. 8 Classification Matrix

True Positives (TP) - These are the correctly predicted positive values, which means that the value of actual class is yes, and the value of predicted class is also yes.

True Negatives (TN) - These are the correctly predicted negative values, which means that the value of actual class is no and the value of predicted class is also no.

False Positives (FP) – This happens when the actual class is no and the predicted class is yes.

False Negatives (FN) – This happens when the actual class is yes but the predicted class is no.

The performance metrics are defined as follows:

- Accuracy: The overall accuracy of a model predicts how well the data has been classified. Accuracy is the most intuitive performance measure and it is simply a ratio of the number of correctly predicted observations to the total number of observations.

$$Accuracy = TP + TN/(TP + FP + FN + TN) \quad (4.2)$$

- Precision: Precision is the ratio of correctly predicted positive observations to the total predicted positive observations. High precision relates to the low false positive rate.

$$Precision = TP/(TP + FP) \quad (4.3)$$

- Recall (Sensitivity): Recall is the ratio of correctly predicted positive observations to all the all observations in actual class.

$$Recall = TP/(TP + FN) \quad (4.4)$$

- F1 score: F1 Score is the weighted average of Precision and Recall. Therefore, this score takes both false positives and false negatives into account.

$$F1\ Score = 2 * (Recall * Precision) / (Recall + Precision) \quad (4.5)$$

4.7 Simulation and Results

To create the database, both secure and insecure cases have been simulated using TSAT software [52] in accordance with the following steps:

1. Generation of Simulation Cases: Multiple '$N-1$' and '$N-k$' contingencies have been simulated in this study. The contingencies are three-phase line to ground faults located at 10% of the distance of the line from the "from" bus. The maximum value of k was 6; so, the largest contingency simulated was opening of 6 lines at the same instant.
2. Measurement of Voltage Magnitude and Voltage Angles: The data to be fed into the different learning algorithms comprise of the bus voltage magnitude in per unit and bus

voltage angle in degrees. It is assumed that PMUs are installed on multiple locations in the system under study and the voltage angle measurements of the buses are provided by them. Based on the PMU placement formulation discussed in (Section 2.2), we determine the locations of buses where the PMUs are to be placed to ensure the system is completely observed.

3. Training Database: After the simulation is carried out for all the N_{OC}, the values are fed into the different machine learning algorithms. Each of these cases are labeled as 1 [secure] or 0 [insecure], before feeding them into the respective learning algorithms. This data serves as the training database for the different techniques.
4. Testing Database: In order to test the ML models built in the previous step, realistic measurements are replicated through introduction of measurement errors in the training database of true voltage phase angles. Additive error model is used which includes both PMU and instrumentation channel errors in the range [86]:
    - PMU errors in phase angles are assumed to be a Gaussian distribution with zero mean and standard deviation of 0.104°.
    - Instrumentation channel errors in phase angle are assumed to be in the range of $\pm 3^{\circ}$, $\pm 2^{\circ}$and $\pm 1^{\circ}$.The measurements considered for the testing purpose are assumed to have a uniform distribution zero mean and standard deviation of 0.1°.

Resultant voltage phase angles after inclusion of additive PMU and instrumentational channel errors [87], [88] is given by:

$$\emptyset_{actual}^{v} = \emptyset_{true}^{v} + \emptyset_{error}^{c} + \emptyset_{error}^{PMU} \tag{4.6}$$

Where $\emptyset_{actual}^{v}$ is the resultant voltage phase angle after incorporation of errors in the true voltage phase angle measurements $\emptyset_{true}^{v}$.The instrumentation channel error is $\emptyset_{error}^{c}$ and PMU error is

$\emptyset_{error}^{PMU}$.

4.7.1 Importance of considering Seasonal Load Modeling:

In this study a seasonal load modeling has been performed to take into consideration the varying load profiles that occurs in different seasons. The importance of this study has been highlighted below by the presentation of three cases, namely, Case 1, Case 2 and Case 3. The results have also been tabulated in Table 4.1.

Case 1 ($N-3$ contingency case):

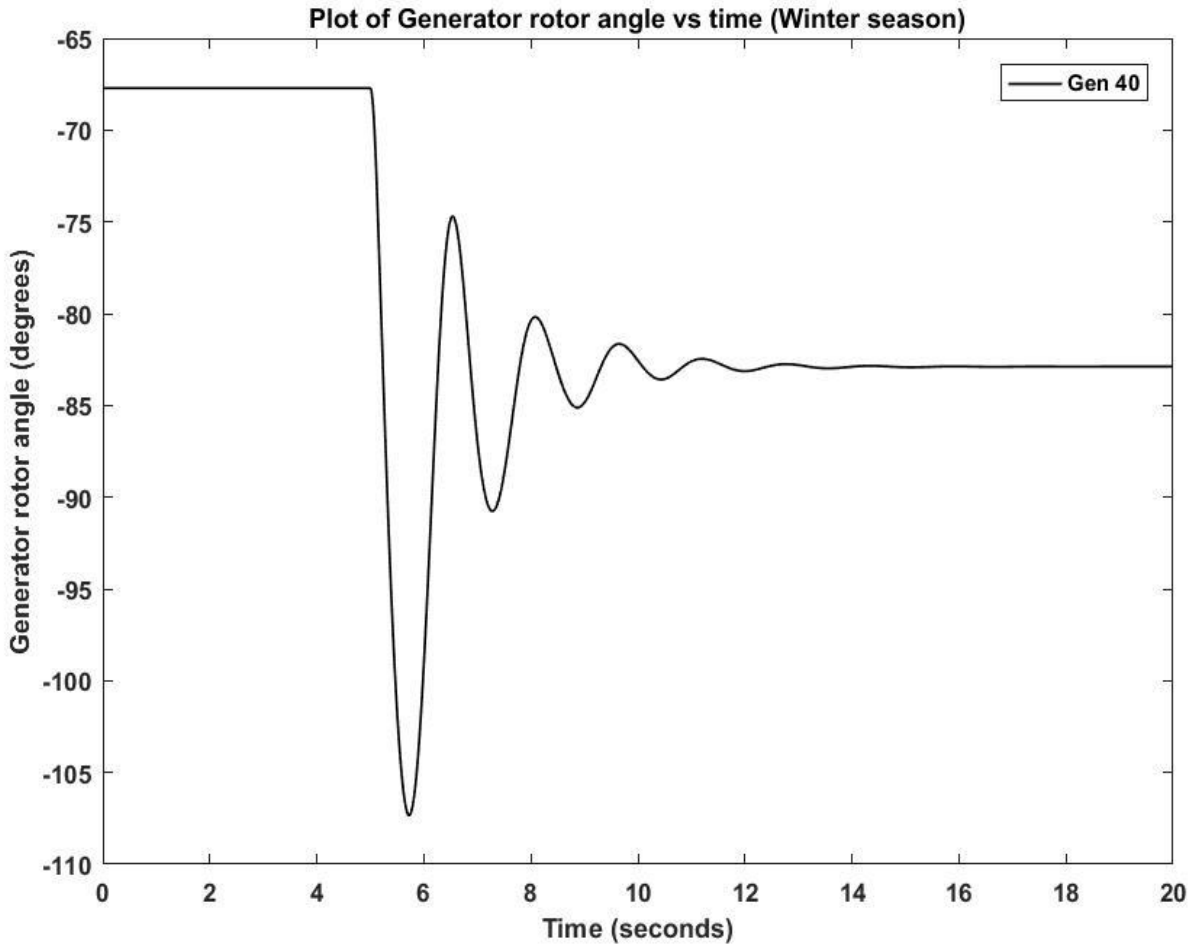

Figure 4. 9 Plot of generator rotor angle at bus number 40 on a winter load profile

In this case, a $N-3$ contingency (3 three-phase line to ground faults) was initiated at 5 seconds

and the simulation was run for 20 seconds. The lines on which fault occurred were 65-64, 38-65, and 37-39. Fig. 4.9 represents the generator rotor angle of bus number 40 for a winter load profile while Fig. 4.10 represents the generator rotor angle of bus number 40 for a summer load p

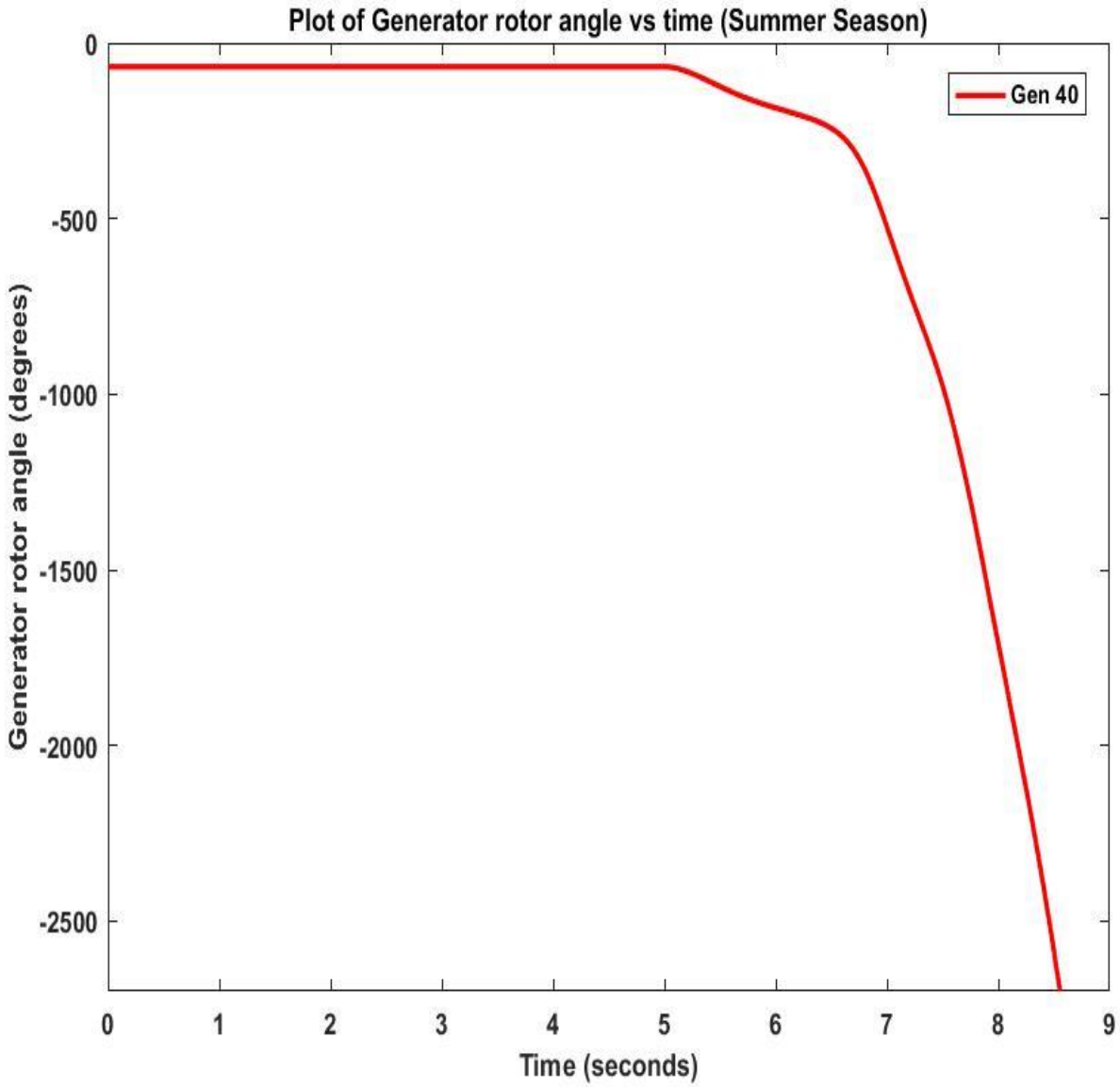

Figure 4. 10 Plot of generator rotor angle at bus number 40 on a summer load profile

It can be observed from the above figures that for a summer load profile (Fig. 4.10), the rotor angle

of generator 40 was swinging away from the system and the simulation lasted for only 8.6 seconds which led the system to becoming transient unstable. Conversely, the system was transient stable (Fig. 4.9) during the winter load profile for the same contingency case.

Case 2 ($N-4$ contingency case):

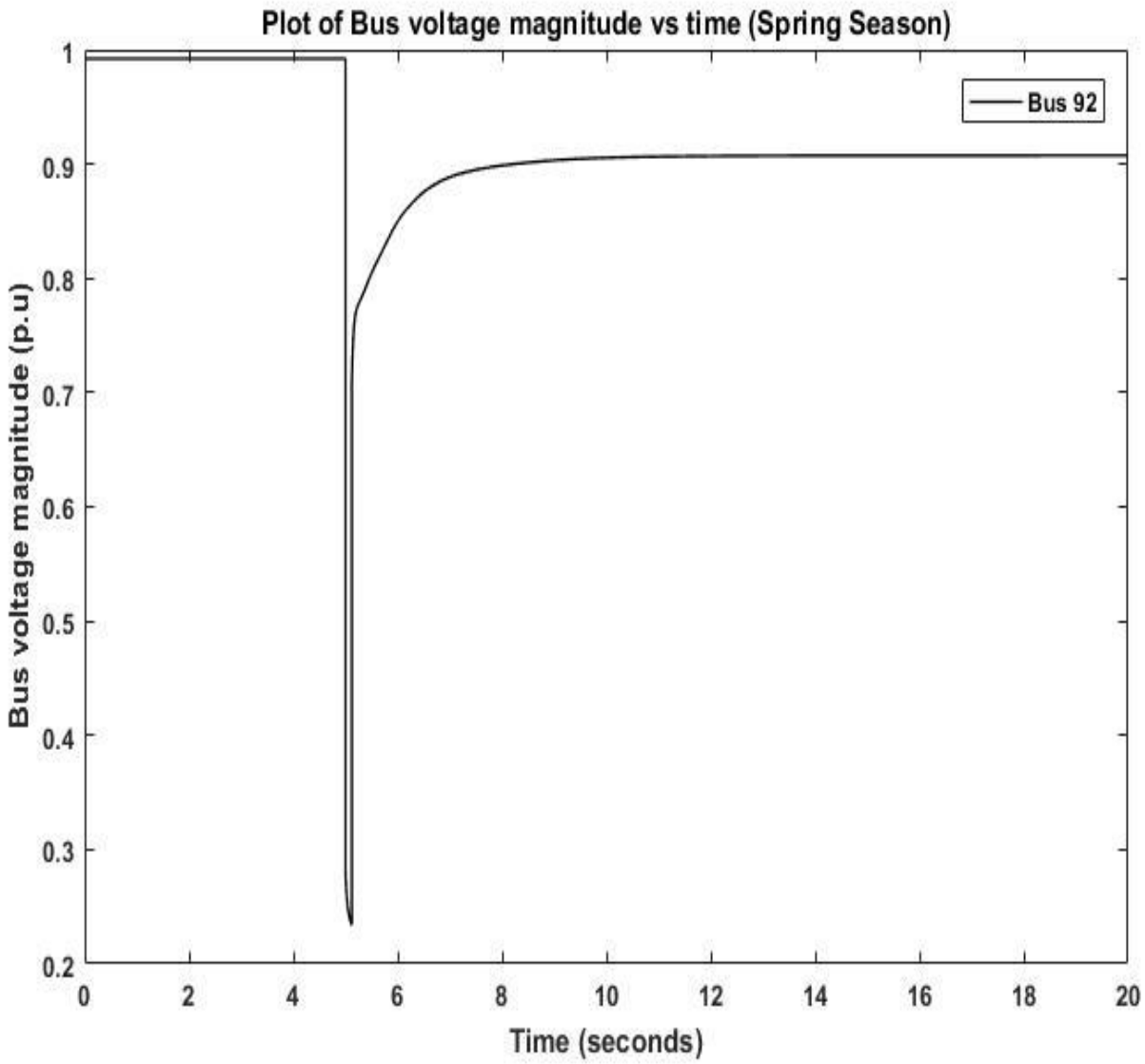

Figure 4. 11 Plot of bus voltage magnitude at bus number 92 on a spring load profile

In this case, a $N-4$ contingency (4 three-phase line to ground faults) was initiated at 5 seconds

and the simulation was run for 20 seconds. The lines on which fault occurred were 93-94, 92-102, 94-96, and 103-104. Fig. 4.11 represents the bus voltage magnitude at bus number 92 for a spring load profile, while Fig. 4.12 represents the bus voltage magnitude at bus number 92 for a fall load profile.

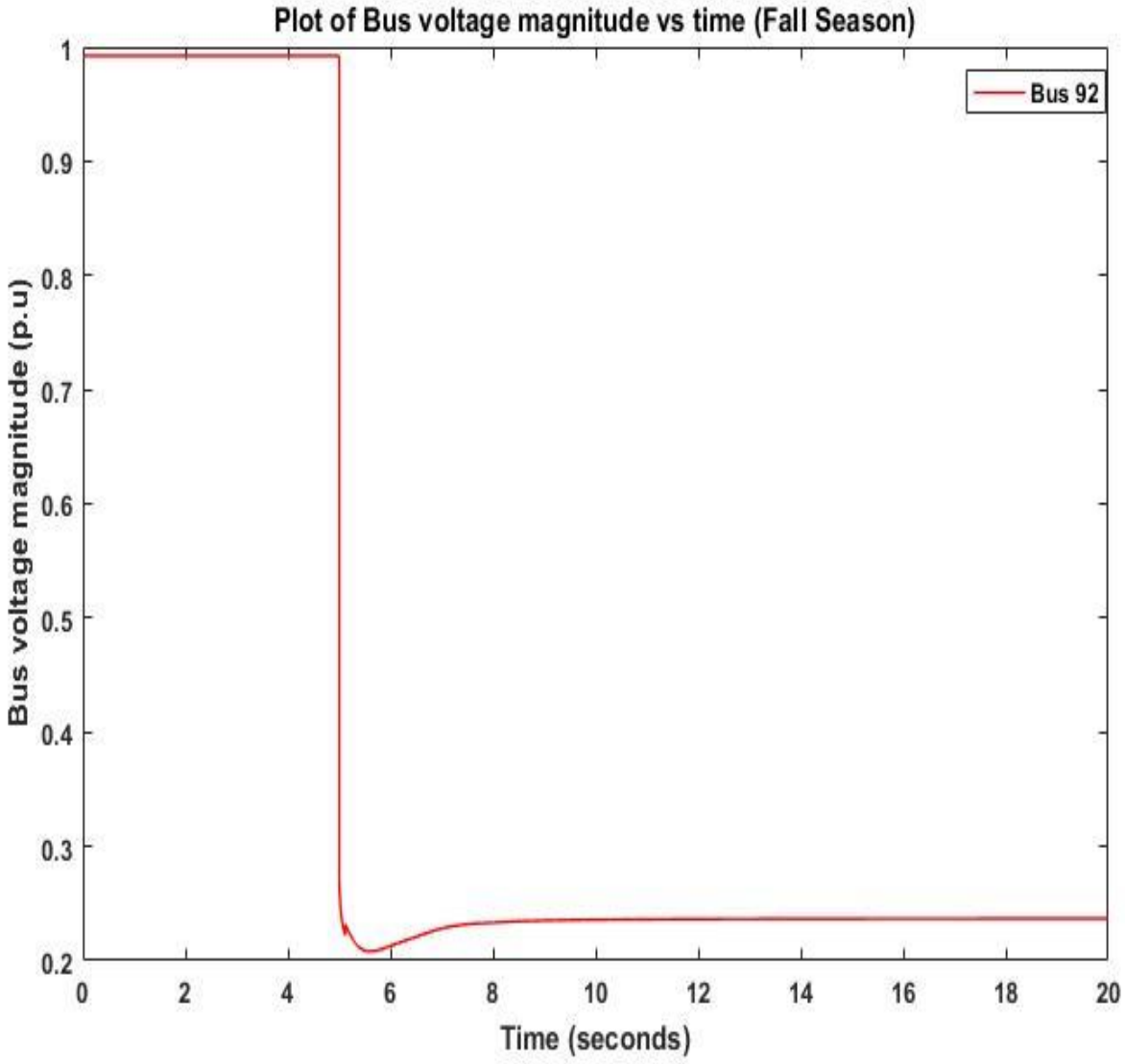

Figure 4. 12 Plot of bus voltage magnitude at bus number 92 on a fall load profile

It can be observed from the above figures that the voltage at bus number 92 suffered a short-term voltage insecurity for a fall load profile (Fig. 4.12) whereas the bus voltage recovered after the

initial dip in case of a spring load profile (Fig. 4.11) for the same applied case.

Case 3 ($N-3$ contingency case):

In Case 3, a $N-3$ contingency (3 three-phase line to ground faults) was initiated at 5 seconds. The faulted lines were as follows 100-101, 103-105, and 103-104. Fig. 4.13 represents the generator rotor angle of bus number 103 for a winter load profile while Fig. 4.14 represents the generator rotor angle of bus number 103 for a summer load profile.

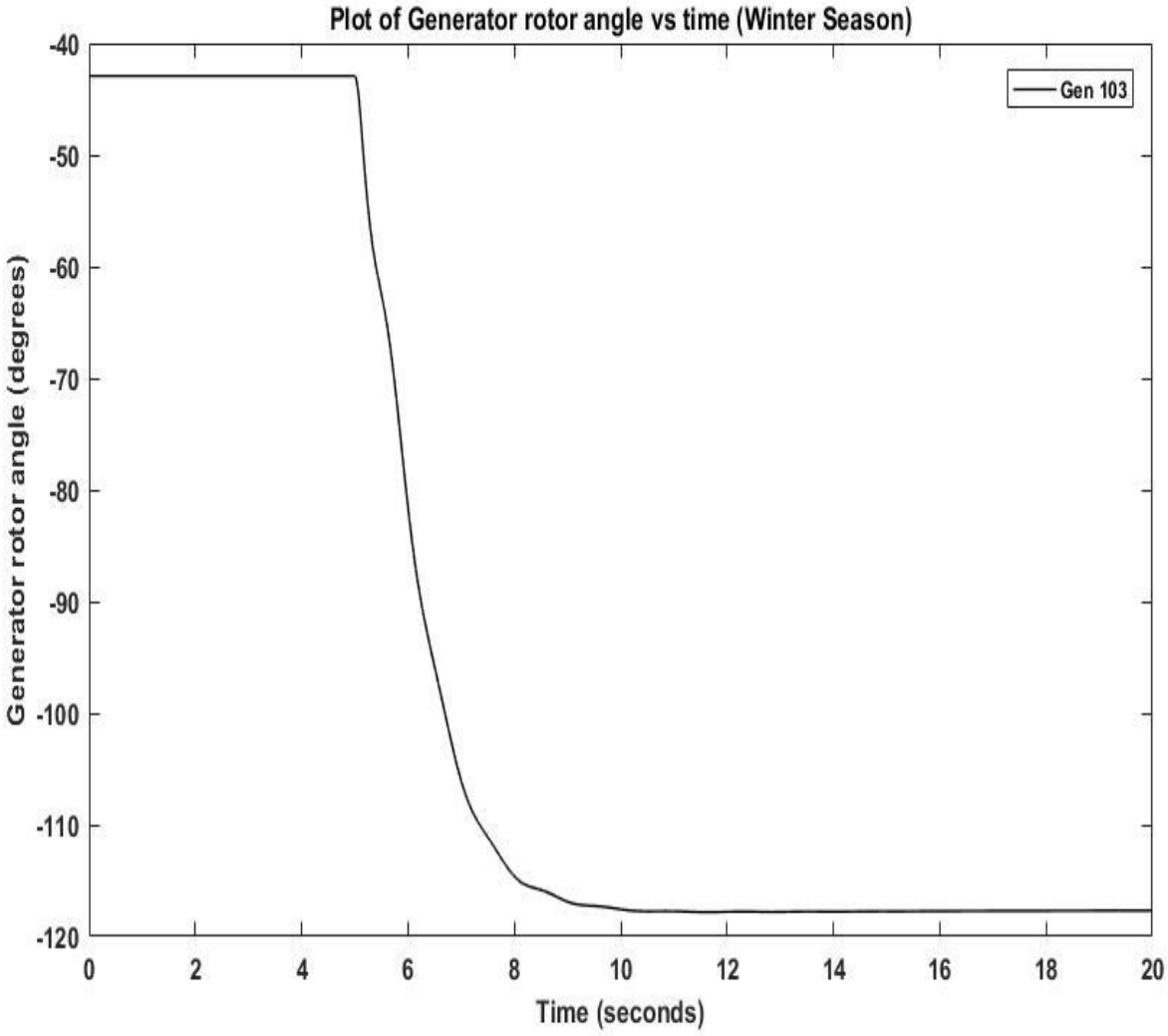

Figure 4. 13 Plot of generator rotor angle at bus number 103 on a winter load profile

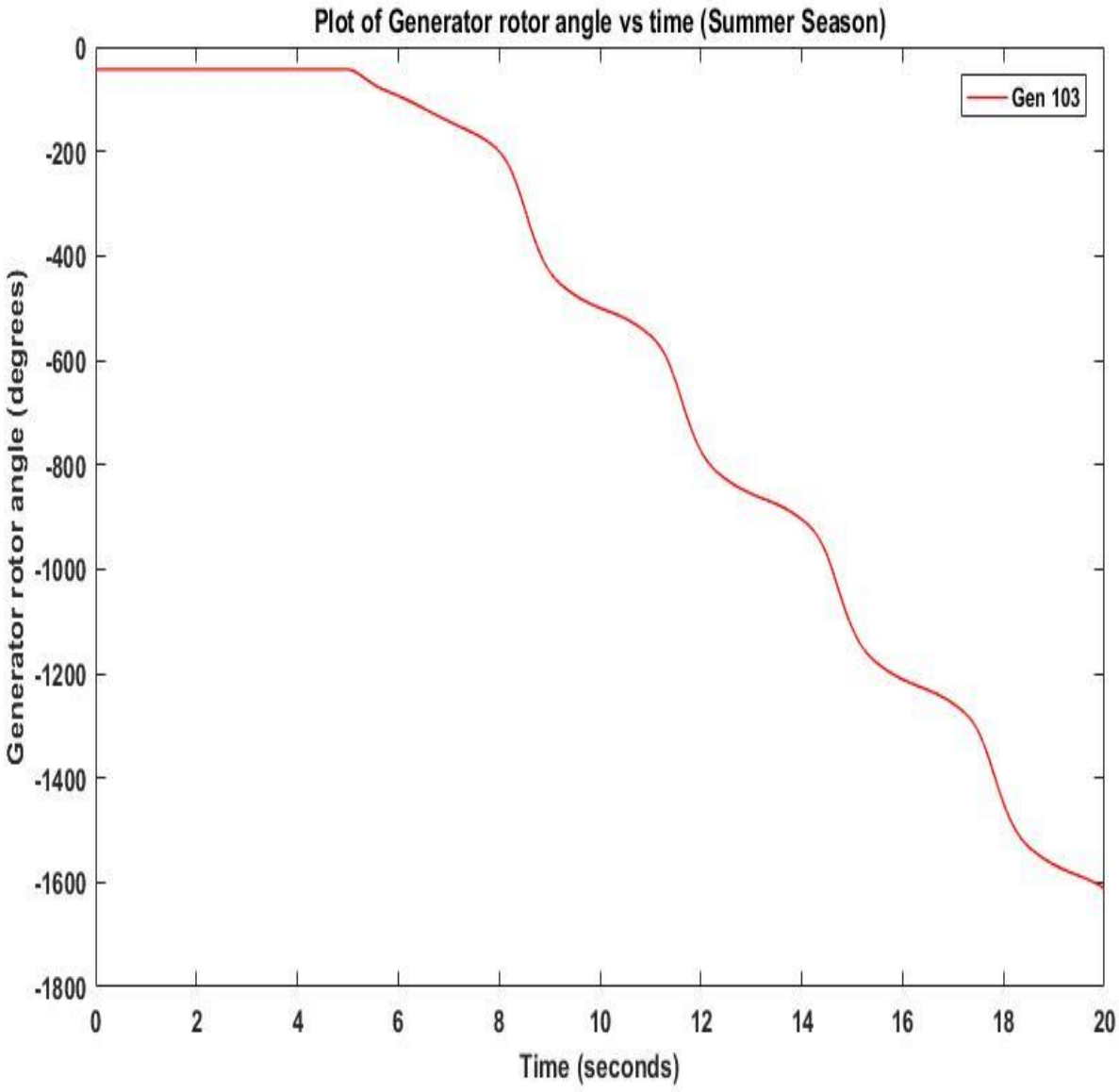

Figure 4. 14 Plot of generator rotor angle at bus number 103 on a summer load profile

From Figure 4.14, it can be observed the generator rotor angle on bus number 103 kept swinging away from the system leading the system to become transient unstable for the summer load profile. Conversely, the rotor angle for the same generator after an initial dip settles down to a stable operating condition after some time for the winter load profile (Fig. 4.13).

Table 4.1 is used to highlight the cases which have been discussed above. From the above case studies, we can justify the need for a seasonal based load modeling wherein for the same contingency, violations occur differently for each season.

Table 4. 1 Comparison of contingency cases across different seasons

Comparative Case Study	Season Result (A)	Season Result (B)	Type of Instability
Case 1 (N-3 contingency) Lines (65-64,38-65 and 37-39)	Winter (Secure)	Summer (Insecure)	Transient Unstable
Case 2 (N-2 contingency) Lines (93-94, 92-102, 94-96, and 103-104.)	Fall (Insecure)	Spring (Secure)	Short term Voltage Unstable
Case 3 (N-3 contingency) Lines (100-101,103-105 and 103-104)	Winter (Secure)	Summer (Insecure)	Transient Unstable

4.7.2 Importance of considering inverter based solar PV penetration in a DSA scheme:

In this study, varying levels of solar penetration have been considered while performing DSA. The importance of this study is to find out the difference in violations that occur with and without the presence of solar PV in the grid. The differences have been highlighted by the presentation of two cases, namely, Case A and Case B. The results have also been tabulated in Table 4.2.

Case A ($N-2$ contingency case):

In Case A, a $N-2$ contingency (2 three-phase line to ground faults) was initiated at 5 seconds. The faulted lines were as follows 103-105 and 103-110. Fig. 4.15 represents the bus voltage magnitude of bus number 111 for a system without solar PV while Fig. 4.16 represents the bus voltage magnitude of bus number 111 for a system with solar PV. The solar PV was installed by replacing the conventional generation at bus number 103 and the variations of voltage at a bus in the vicinity of 103 was plotted.

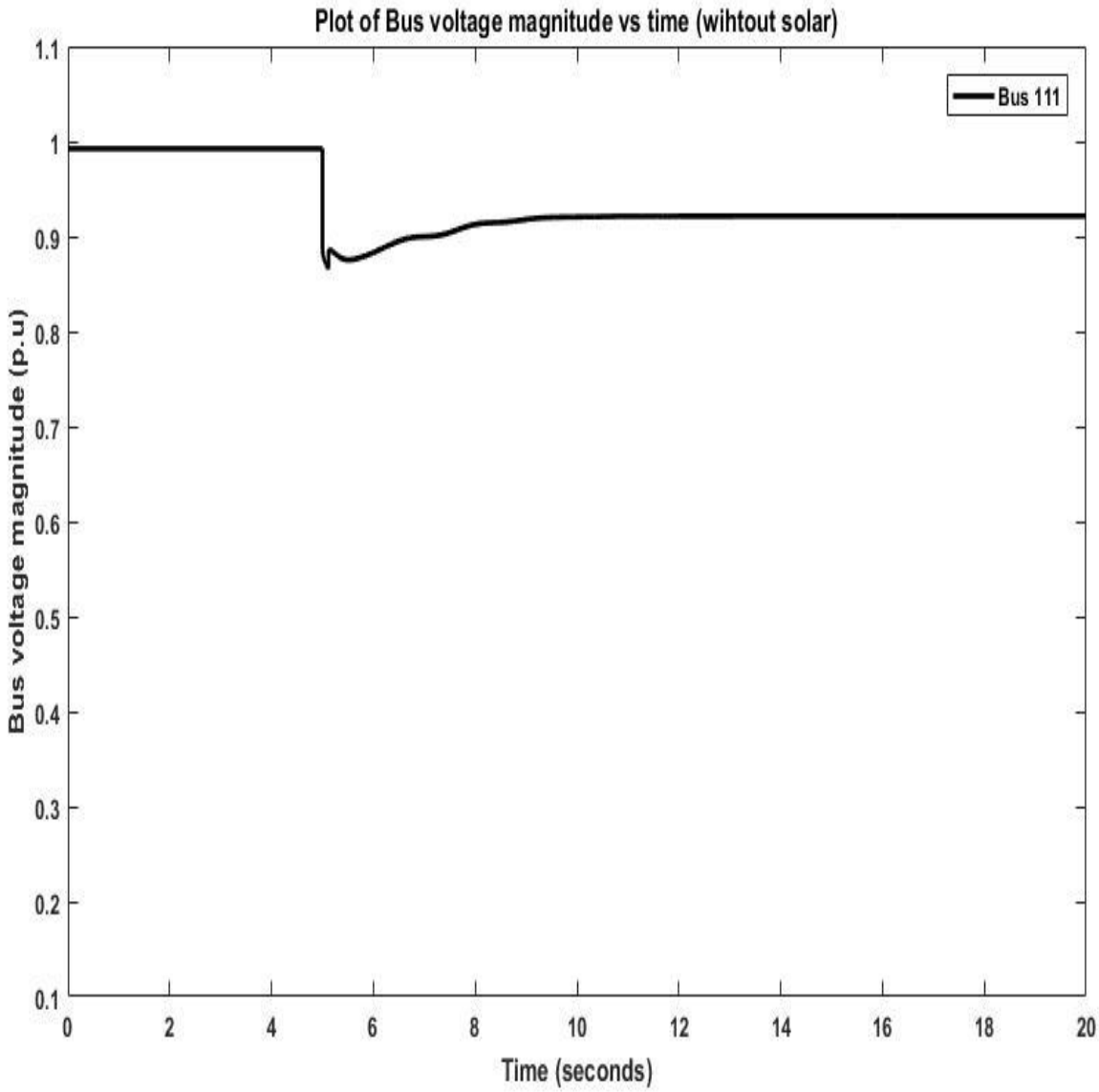

Figure 4. 15 Plot of bus voltage magnitude at bus number 111 (without solar PV)

It can be observed in this case that when solar PV is installed in the system, there is a violation of short-term voltage security for the same contingency case. In Fig. 4.16, we observe that the bus voltage at bus number 111 has failed to recover to a stable value following a contingency because of the presence of solar PV on a neighboring bus.

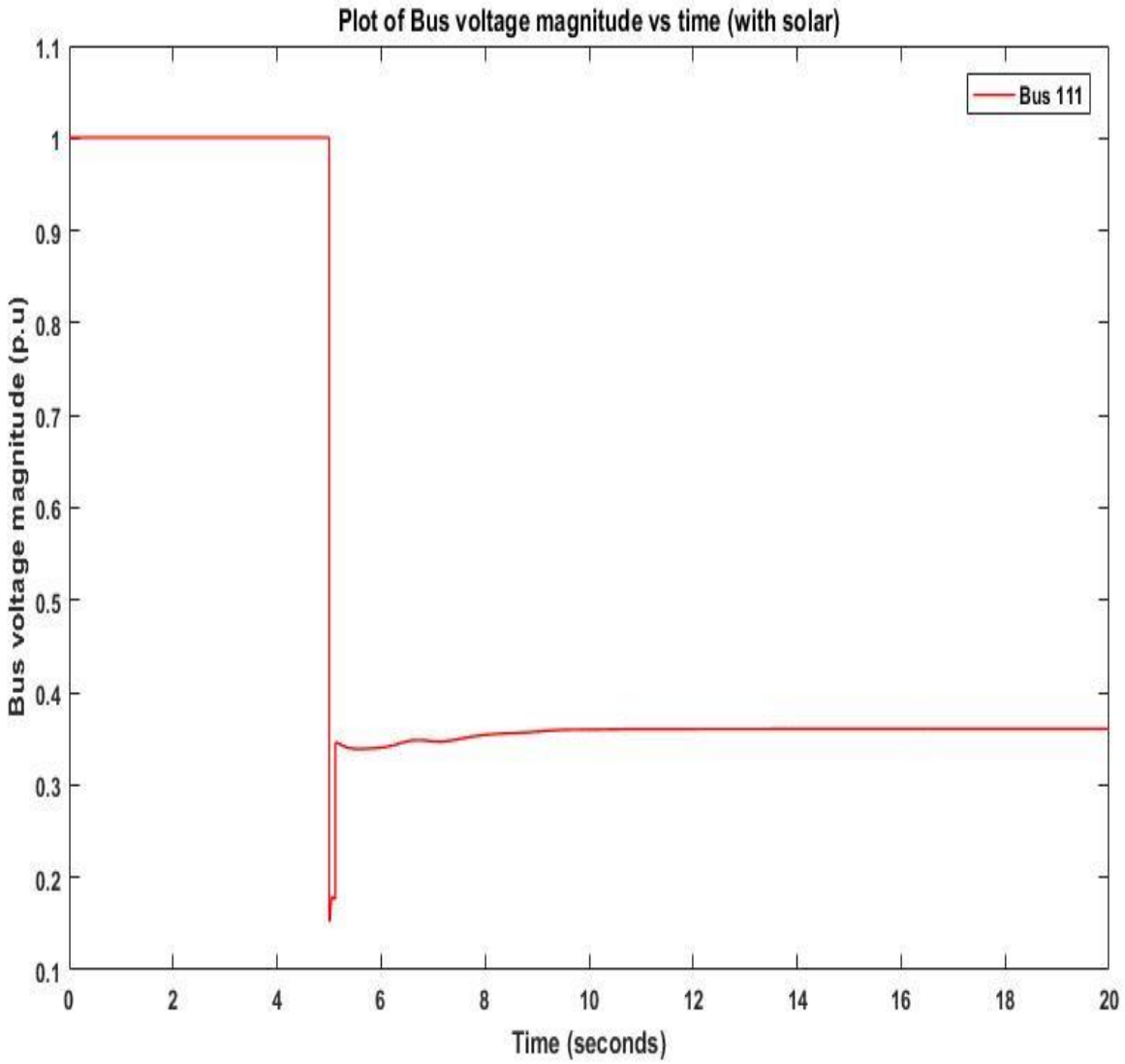

Figure 4. 16 Plot of bus voltage magnitude at bus number 111 (with solar PV)

Case B ($N-2$ contingency case): In Case C, a $N-2$ contingency (2 three-phase line to ground faults) was initiated at 5 seconds. The faulted lines were 54-56 and 54-59. Fig. 4.19 represents the bus voltage magnitude of bus number 56 for a system without solar PV while Fig. 4.20 represents the bus voltage magnitude of bus number 56 for a system with solar PV. The solar PV was installed

by replacing the conventional generation at bus number 54 and the variation of voltage at a bus in the vicinity of 54 was plotted.

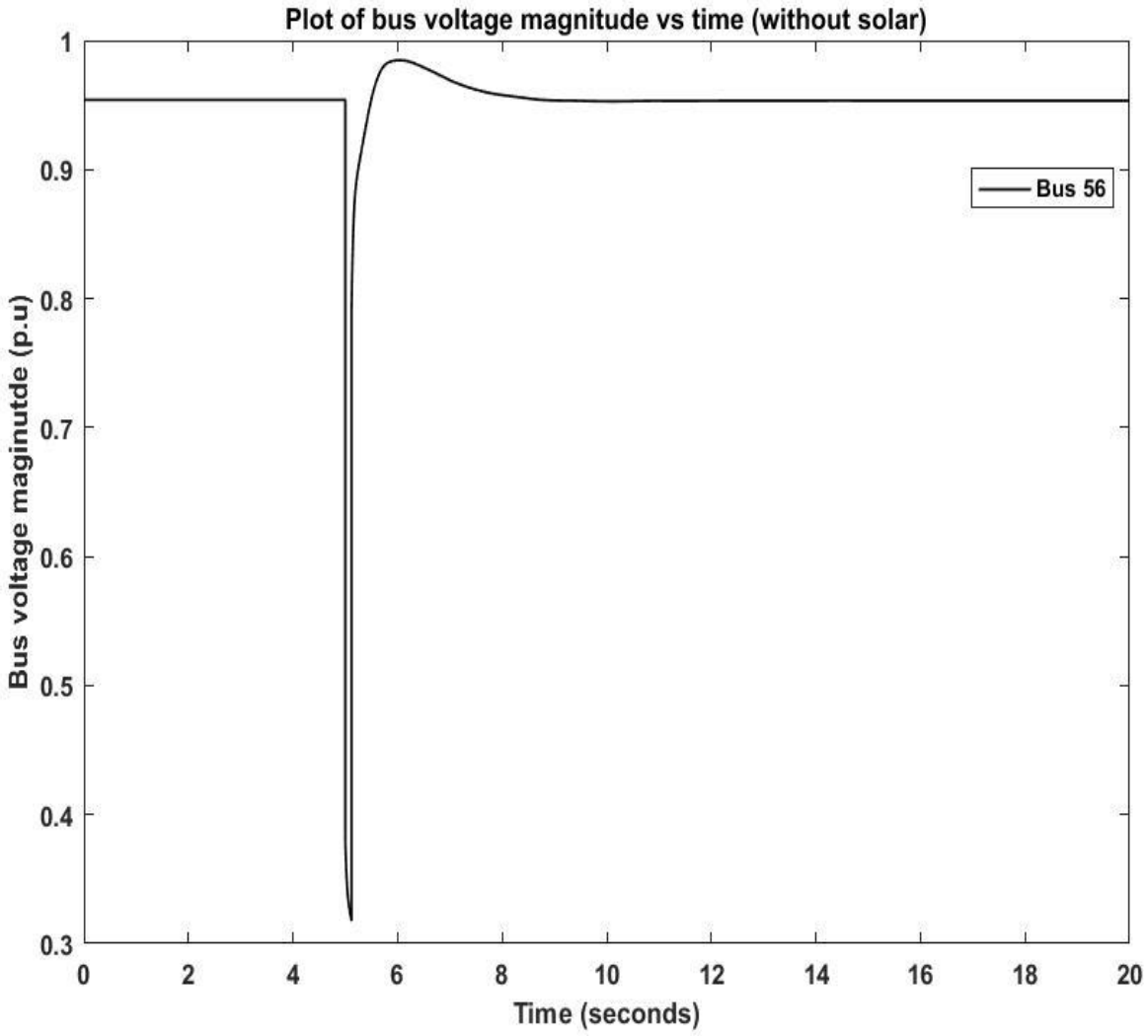

Figure 4. 17 Plot of bus voltage magnitude at bus number 56 (without solar PV)

We again observe that following a contingency, there is a violation in voltage at bus number 56 (Fig. 4.20) when solar PV has been installed at bus number 54, while there is no violation in a system without the presence of solar PV. The voltage at bus number 56 rises to a stable value (see Fig. 4.19) after the initial dip when solar generation has not been integrated in the system.

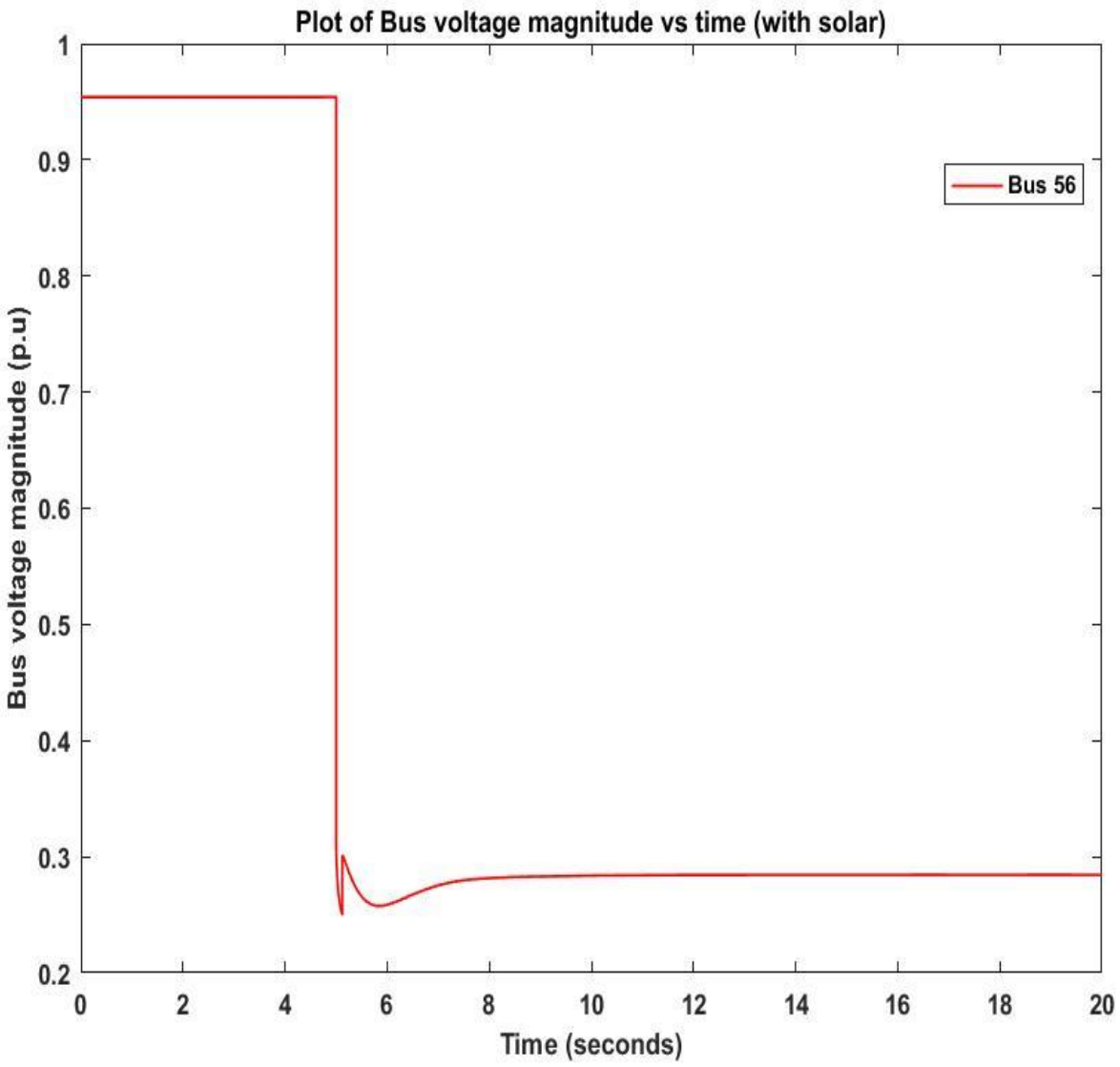

Figure 4. 18 Plot of bus voltage magnitude at bus number 56 (with solar PV)

Table 4.2 is used to highlight the cases which have been discussed above. From the above case studies, we observe that there is a significant difference in the number of violations that occur in a system with and without inverter based solar PV generation. Therefore, it is critical to include solar PV while developing a DSA scheme.

Table 4. 2 Comparison of contingency cases with and without solar integration

Comparative Case Study	Without Solar PV	With Solar PV
Case A (N-2 contingency) Lines (103-105 and 103-110)	Secure	Insecure
Case B (N-3 contingency) Lines (54-56 and 54-59)	Secure	Insecure

4.7.3. Results for Summer Daily Load Case:

A total of 4,800 cases were generated for the summer load profile out of which 1,780 cases were insecure and the remaining 3,020 cases were secure. The database is then fed to different algorithms to try and classify the security of the system. The results of the different ML algorithms are as follows:

Table 4. 3 Summary of results for DT testing accuracies for Summer Season considering measurement errors

Error		DT
Systematic Error	**Random Error**	**Accuracy (%)**
0	0 Mean ±0.104SD	99.59±0.00
0 Mean ± 0.1SD		93.21±0.25
±1		85.40±0.82
±2		77.42±1.46
±3		72.09±1.75

Table 4. 4 Summary of results for SVM testing accuracies for Summer Season considering measurement errors

Error		SVM			
Systematic Error	**Random Error**	**Accuracy (%)**	**Precision**	**Recall**	**F1-score**
0	0 Mean ±0.104 SD	97.10 ± 0.00	0.9708	0.9729	0.9725
0 Mean ± 0.1SD		94.05 ± 0.22	0.9452	0.9434	0.9438
±1		92.40 ± 0.53	0.9231	0.9285	0.9298
±2		90.20 ± 0.80	0.9032	0.9122	0.9022
±3		89.99 ± 1.30	0.8998	0.8951	0.8925

Table 4. 5 Summary of results for RF testing accuracies for Summer Season considering measurement errors

Error		RF			
Systematic Error	**Random Error**	**Accuracy (%)**	**Precision**	**Recall**	**F1-score**
0	0 Mean ±0.104 SD	99.8 ± 0.00	0.9928	0.9975	0.9929
0 Mean ± 0.1SD		92.98 ± 0.44	0.9245	0.9284	0.9240
±1		87.22 ± 0.68	0.8791	0.8764	0.8740
±2		78.24 ± 1.18	0.7829	0.7812	0.7928
±3		73.45 ± 1.42	0.7356	0.7380	0.7402

Table 4. 6 Summary of results for MLNN testing accuracies for Summer Season considering measurement errors

Error		MLNN			
Systematic Error	**Random Error**	**Accuracy (%)**	**Precision**	**Recall**	**F1-score**
0	0 Mean ±0.104 SD	97.80 ± 0.00	0.9798	0.9825	0.9840
0 Mean ± 0.1SD		93.12 ± 0.34	0.9325	0.9348	0.9366
±1		91.67 ± 0.75	0.9182	0.9188	0.9125
±2		89.21 ± 0.92	0.8926	0.8922	0.8923
±3		87.52 ± 1.84	0.8821	0.8702	0.8715

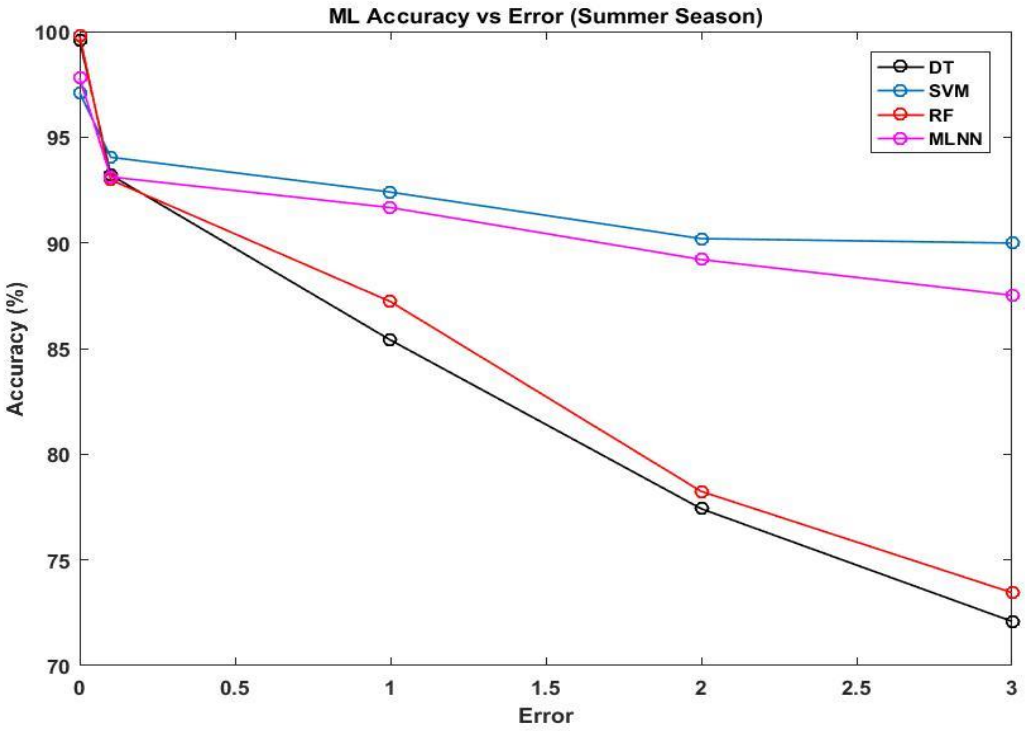

Figure 4. 19 Plot of ML Accuracy vs Error for Summer Daily load profile

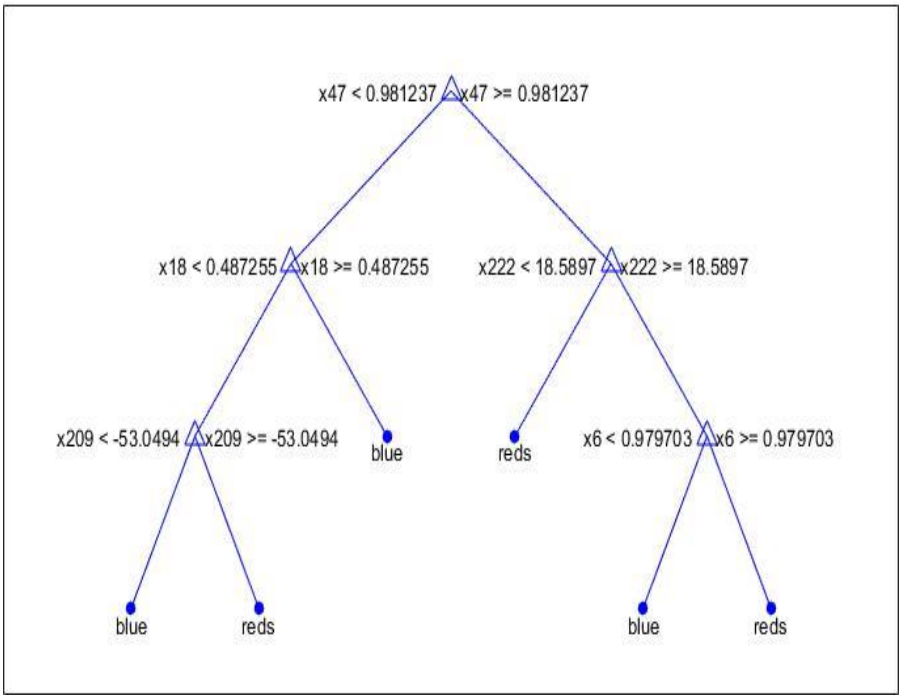

Figure 4. 20 DT results for Summer Daily load profile

From four tables given above (Tables 4.3-4.6) and Fig.4.19 we observe that performance of RF without the presence of errors is better than the other algorithms closely followed by DT. With the presence of errors, the performance of SVM is superior in comparison with the other techniques. In Fig. 4.20, “blue” terminal nodes indicate secure and “reds” terminal nodes indicate insecure.

4.7.4 Results for Spring Daily Load Case:

A total of 4,800 cases were generated for the spring load profile out of which 1,320 cases were insecure and the remaining 3,480 cases were secure. The database is then fed to different algorithms to try and classify the security of the system. The results of the different ML algorithms are as follows:

Table 4. 7 Summary of results for DT testing accuracies for Spring Season considering measurement errors

Error		**DT**
Systematic Error	**Random Error**	**Accuracy (%)**
0	0 Mean ±0.104SD	99.65±0.00
0 Mean ± 0.1SD		92.22±0.31
±1		84.56±0.90
±2		78.55±1.32
±3		71.92±1.52

Table 4. 8 Summary of results for SVM testing accuracies for Spring Season considering measurement errors

Error		SVM			
Systematic Error	**Random Error**	**Accuracy (%)**	**Precision**	**Recall**	**F1-score**
0	0 Mean ±0.104 SD	97.05 ± 0.00	0.9703	0.9722	0.9717
0 Mean ± 0.1SD		93.10± 0.56	0.9320	0.9356	0.9335
±1		92.01 ± 0.72	0.9205	0.9287	0.9223
±2		91.52 ± 1.22	0.9132	0.9115	0.9122
±3		90.01 ± 1.36	0.9092	0.9010	0.9052

Table 4. 9 Summary of results for RF testing accuracies for Spring Season considering measurement errors

Error		RF			
Systematic Error	**Random Error**	**Accuracy (%)**	**Precision**	**Recall**	**F1-score**
0	0 Mean ±0.104 SD	99.78 ± 0.00	0.9998	0.9975	0.9989
0 Mean ± 0.1SD		91.72 ± 0.22	0.9155	0.9173	0.9160
±1		85.43 ± 0.55	0.8593	0.8522	0.8555
±2		76.92 ± 0.99	0.7630	0.7698	0.7662
±3		72.98 ± 1.26	0.7291	0.7295	0.7293

Table 4. 10 Summary of results for MLNN testing accuracies for Spring Season considering measurement errors

Error		MLNN			
Systematic Error	**Random Error**	**Accuracy (%)**	**Precision**	**Recall**	**F1-score**
0	0 Mean ±0.104 SD	97.42 ± 0.00	0.9798	0.9625	0.9740
0 Mean ± 0.1SD		92.01 ± 0.34	0.9256	0.9241	0.9248
±1		90.12 ± 0.75	0.9099	0.9015	0.9052
±2		88.15 ± 0.92	0.8819	0.8892	0.8864
±3		87.91 ± 1.34	0.8725	0.8778	0.8769

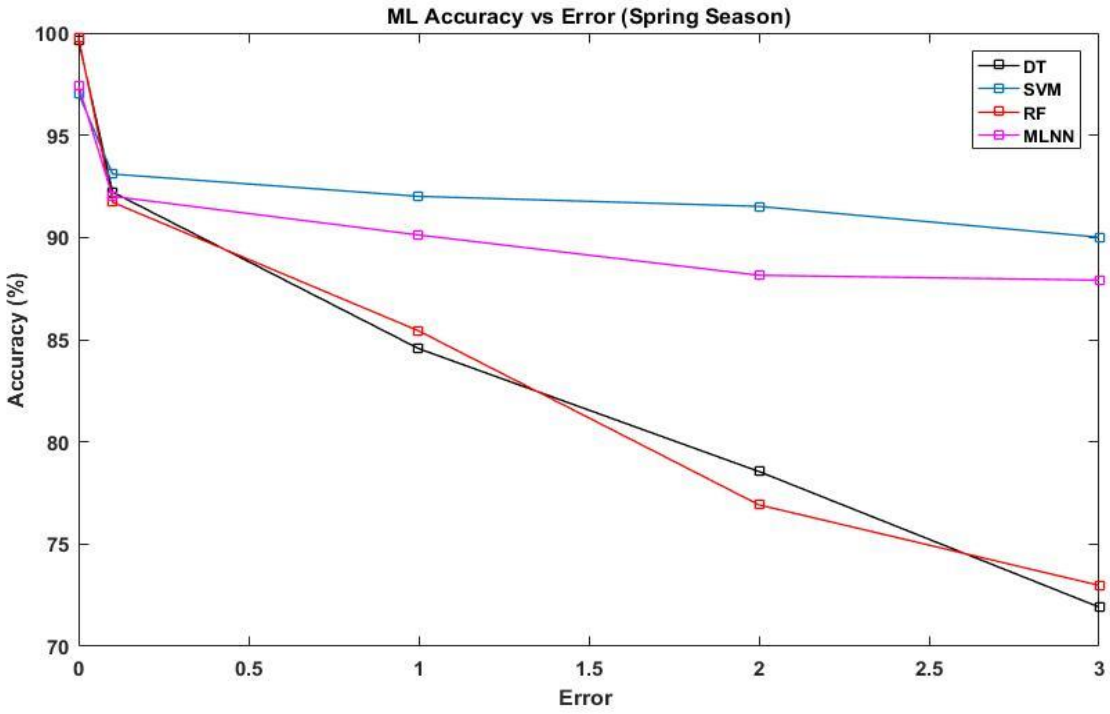

Figure 4. 21 Plot of ML Accuracy vs Error for Spring Daily load profile

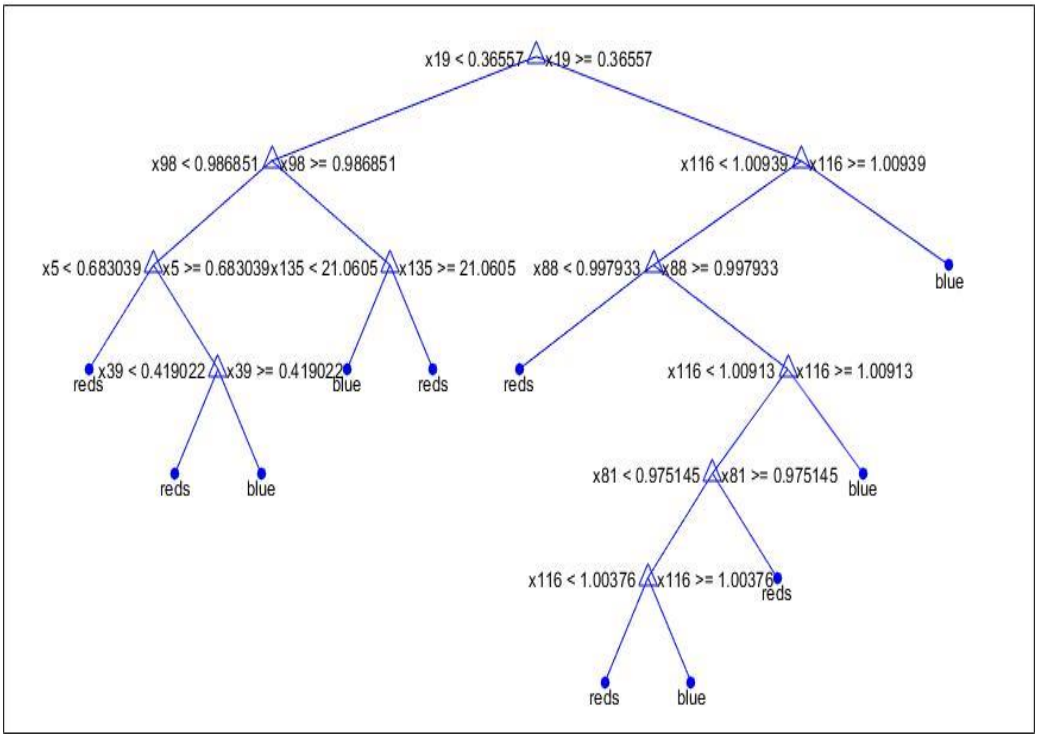

Figure 4. 22 DT results for Spring Daily load profile

From the above tables (Tables 4.7-4.10) and Fig. 4.21 we arrive at the conclusion that without errors the performance of RF is better than other algorithms closely followed by DT. With the addition of errors, SVM has the highest accuracy and its performance is better than all the other algorithms. In Fig. 4.22, DT results for Spring load profile have been plotted wherein the "blue" terminal nodes indicate secure and "reds" terminal nodes indicate insecure.

4.7.5 Results for Fall Daily Load Case:

A total of 4,800 cases were generated for the fall load profile out of which 1,510 cases were insecure and the remaining 3,290 cases were secure. The database is then fed to different algorithms to try and classify the security of the system. The results of the different ML algorithms are as follows:

Table 4. 11 Summary of results for DT testing accuracies for Fall Season considering measurement errors

Error		**DT**
Systematic Error	**Random Error**	**Accuracy (%)**
0	0 Mean ±0.104SD	98.20±0.00
0 Mean ± 0.1SD		91.94±0.62
±1		85.31±0.52
±2		77.63±1.59
±3		69.98±1.78

Table 4. 12 Summary of results for SVM testing accuracies for Fall Season considering measurement errors

Error		SVM			
Systematic Error	**Random Error**	**Accuracy (%)**	**Precision**	**Recall**	**F1-score**
0	0 Mean ±0.104 SD	97.22 ± 0.00	0.9708	0.9729	0.9725
0 Mean ± 0.1SD		92.55± 0.56	0.9255	0.9278	0.9263
±1		91.52 ± 0.72	0.9151	0.9232	0.9178
±2		90.78 ± 1.22	0.9097	0.9078	0.9102
±3		90.02 ± 1.36	0.9091	0.9022	0.9055

Table 4. 13 Summary of results for RF testing accuracies for Fall Season considering measurement errors

Error		RF			
Systematic Error	**Random Error**	**Accuracy (%)**	**Precision**	**Recall**	**F1-score**
0	0 Mean ±0.104 SD	99.22 ± 0.00	0.9998	0.9975	0.9989
0 Mean ± 0.1SD		91.31 ± 0.31	0.9122	0.9148	0.9132
±1		86.77 ± 0.61	0.8692	0.8624	0.8655
±2		78.32 ± 0.95	0.7811	0.7892	0.7842
±3		73.55 ± 1.45	0.7390	0.7315	0.7362

Table 4. 14 Summary of results for MLNN testing accuracies for Fall Season considering measurement errors

Error		MLNN			
Systematic Error	**Random Error**	**Accuracy (%)**	**Precision**	**Recall**	**F1-score**
0	0 Mean ±0.104 SD	97.22 ± 0.00	0.9798	0.9825	0.9840
0 Mean ± 0.1SD		92.55 ± 0.34	0.9220	0.9259	0.9242
±1		90.01 ± 0.75	0.9007	0.9056	0.9025
±2		88.28 ± 0.92	0.8815	0.8875	0.8852
±3		85.21 ± 1.34	0.8522	0.8598	0.8572

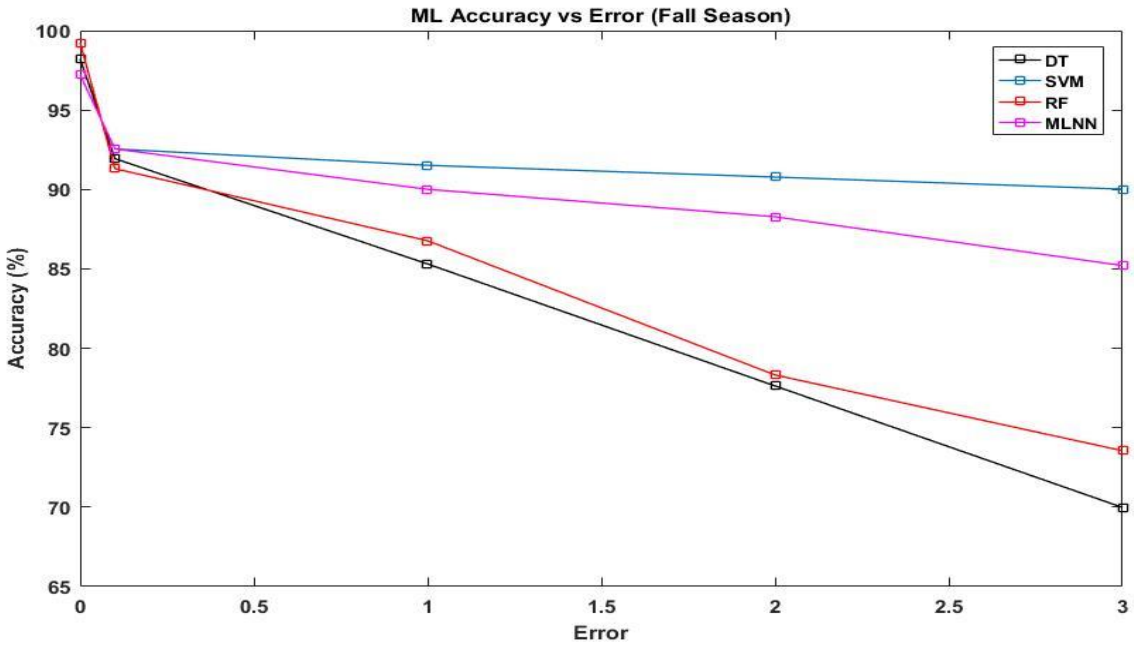

Figure 4. 23 Plot of ML Accuracy vs Error for Fall Daily load profile

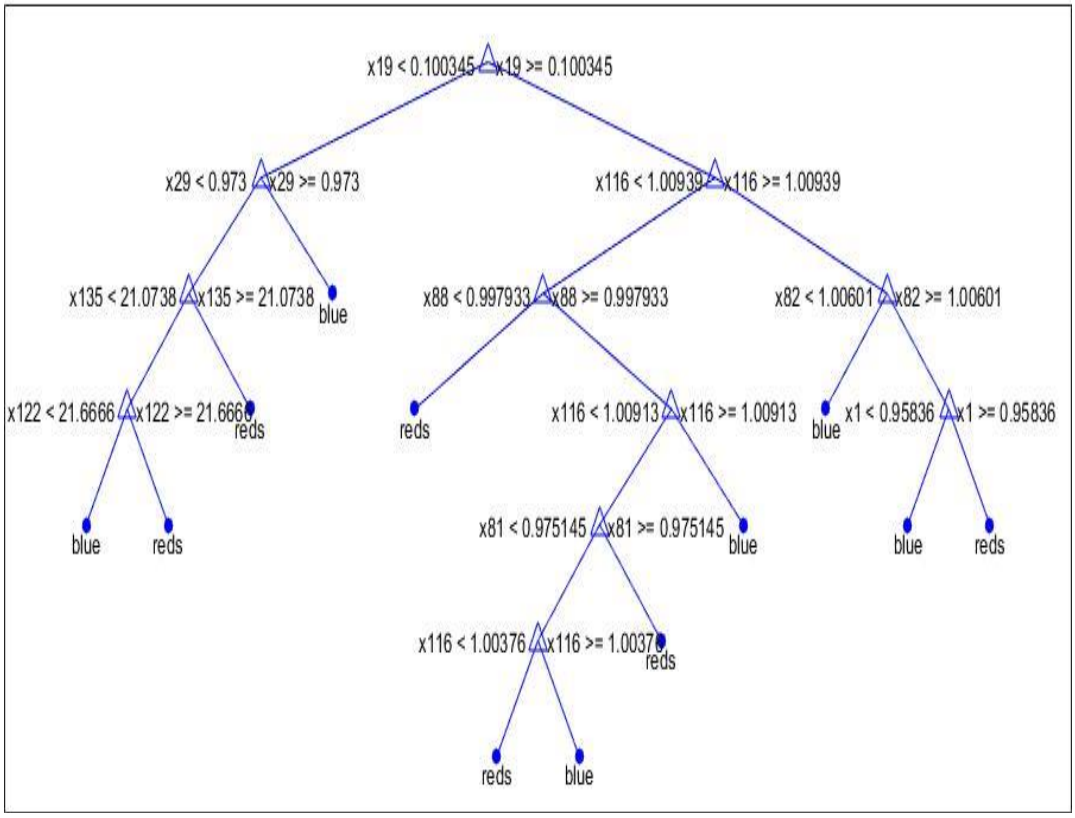

Figure 4. 24 DT results for Fall Daily load profile

From the above tables (Tables 4.11-4.14) and Fig.4.23 we arrive at the conclusion that for fall season the performance of RF is better than other algorithms closely followed by DT without the addition of errors. With the addition of errors, SVM has the highest accuracy and its performance is better than all the other algorithms. Fig. 4.24, represents the DT results for fall daily load profile where the "blue" terminal nodes indicate secure and "reds" terminal nodes indicate insecure points.

4.7.6 Results for Winter Daily Load Case:

Out of the 4,800 cases that were generated for winter load case, 1,392 cases were insecure while the remaining 3,408 cases were found to be secure. The database is then fed to different algorithms to try and classify the security of the system. The results of the different ML algorithms are as follows:

Table 4. 15 Summary of results for DT testing accuracies for Winter Season considering measurement errors

Error		**DT**
Systematic Error	**Random Error**	**Accuracy (%)**
0	0 Mean ±0.104SD	99.68±0.00
0 Mean ± 0.1SD		91.94±0.55
±1		85.31±0.81
±2		77.63±1.21
±3		69.98±1.56

Table 4. 16 Summary of results for SVM testing accuracies for Winter Season considering measurement errors

Error		SVM			
Systematic Error	**Random Error**	**Accuracy (%)**	**Precision**	**Recall**	**F1-score**
0	0 Mean ±0.104 SD	96.95 ± 0.00	0.9708	0.9679	0.9699
0 Mean ± 0.1SD		92.55± 0.51	0.9255	0.9278	0.9263
±1		91.91 ± 0.67	0.9151	0.9132	0.9142
±2		90.77 ± 0.91	0.9092	0.9051	0.9065
±3		90.12 ± 1.01	0.9091	0.9022	0.9055

Table 4. 17 Summary of results for RF testing accuracies for Winter Season considering measurement errors

Error		RF			
Systematic Error	**Random Error**	**Accuracy (%)**	**Precision**	**Recall**	**F1-score**
0	0 Mean ±0.104 SD	99.77 ± 0.00	0.9998	0.9975	0.9989
0 Mean ± 0.1SD		91.23 ± 0.21	0.9122	0.9248	0.9189
±1		84.28 ± 0.55	0.8451	0.8499	0.8478
±2		77.99 ± 0.98	0.7752	0.7791	0.7771
±3		71.68 ± 1.65	0.7156	0.7182	0.7253

Table 4. 18 Summary of results for MLNN testing accuracies for Winter Season considering measurement errors

Error		MLNN			
Systematic Error	**Random Error**	**Accuracy (%)**	**Precision**	**Recall**	**F1-score**
0	0 Mean ±0.104 SD	97.01 ± 0.00	0.9798	0.9825	0.9840
0 Mean ± 0.1SD		93.21 ± 0.51	0.9220	0.9259	0.9242
±1		90.01 ± 0.81	0.9007	0.9056	0.9025
±2		88.28 ± 0.99	0.8815	0.8875	0.8852
±3		86.02 ± 1.78	0.8645	0.8690	0.8661

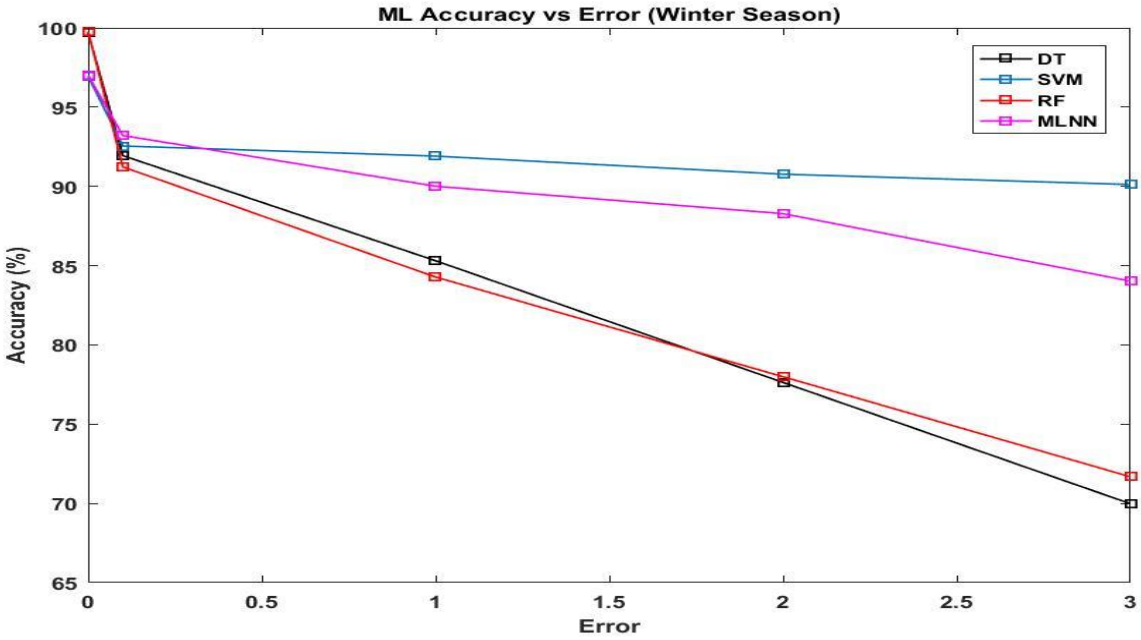

Figure 4. 25 Plot of ML Accuracy vs Error for Winter Daily load profile

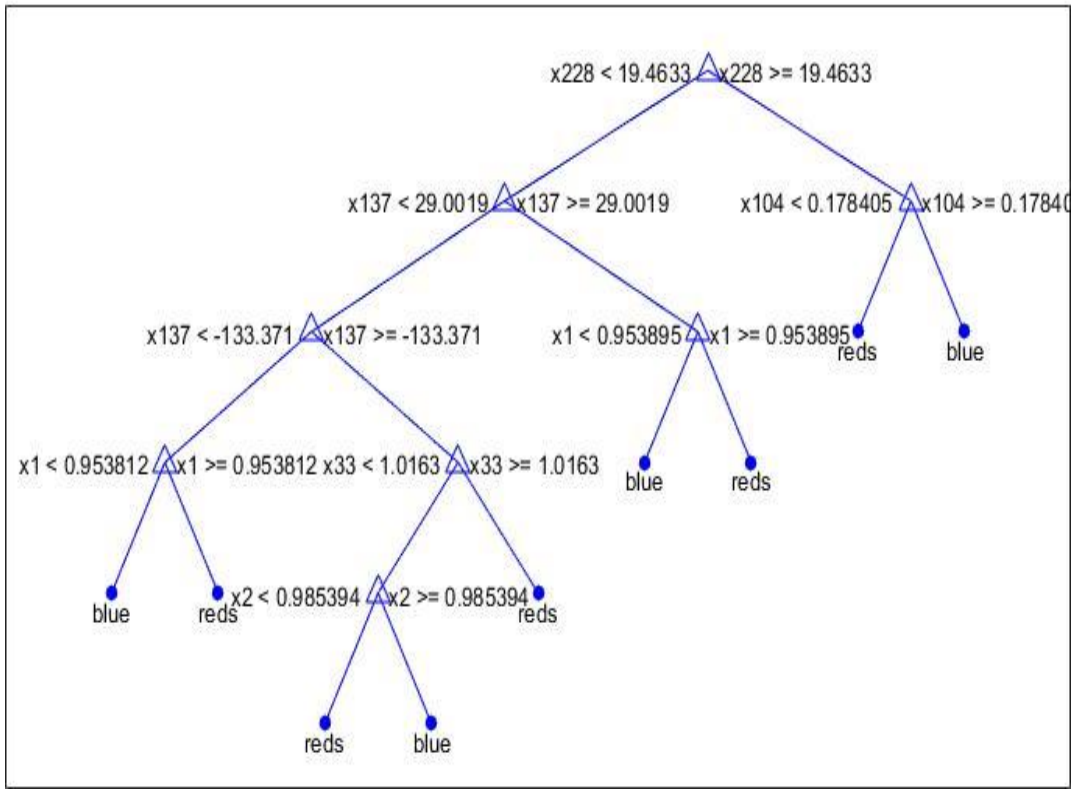

Figure 4. 26 DT results for Winter Daily load profile

From the above tables (Tables 4.15-4.18) and Fig. 4.25 we arrive at the conclusion that for winter season load profile, SVM has the highest accuracy and its performance is better than all the other algorithms with the addition of errors. The performance of RF is better than other algorithms closely followed by DT without the addition of errors. Fig. 4.26, represents the DT results for winter daily load profile wherein the blue" terminal nodes indicate secure and "reds" terminal nodes indicate insecure points.

4.7.7 Results for 10% Solar Penetration Case:

Approximately 10% of the total generation is replaced with solar PV and the accuracy of the scheme is tested on this modified system. The simulations were repeated 75 times and a 95% confidence interval accuracy was computed for the test data with a range of measurement errors. The results obtained are presented below:

Table 4. 19 Summary of results for DT testing accuracies considering 10% solar penetration and measurement error**s**

Error		**DT**
Systematic Error	**Random Error**	**Accuracy (%)**
0	0 Mean ±0.104SD	99.50±0.00
0 Mean ± 0.1SD		91.94±0.62
±1		86.42±0.52
±2		78.99±1.59
±3		70.12±1.98

Table 4. 20 Summary of results for SVM testing accuracies considering 10% solar penetration and measurement error

Error		SVM			
Systematic Error	**Random Error**	**Accuracy (%)**	**Precision**	**Recall**	**F1-score**
0	0 Mean ±0.104 SD	97.03 ± 0.00	0.9708	0.9679	0.9699
0 Mean ± 0.1SD		93.25± 0.65	0.9378	0.9351	0.9364
±1		91.52 ± 0.88	0.9177	0.9192	0.9181
±2		90.59 ± 1.02	0.9053	0.9096	0.9075
±3		89.91 ± 1.52	0.9002	0.8995	0.8998

Table 4. 21 Summary of results for RF testing accuracies for 10% solar penetration and considering measurement errors

Error		RF			
Systematic Error	**Random Error**	**Accuracy (%)**	**Precision**	**Recall**	**F1-score**
0	0 Mean ±0.104 SD	99.52 ± 0.00	0.9998	0.9975	0.9989
0 Mean ± 0.1SD		92.33 ± 0.35	0.9242	0.9266	0.9252
±1		87.51 ± 0.78	0.8761	0.8792	0.8771
±2		79.81 ± 1.11	0.7941	0.7992	0.7960
±3		74.72 ± 1.55	0.7431	0.7502	0.7477

Table 4. 22 Summary of results for MLNN testing accuracies for 10% solar penetration and considering measurement errors

Error		MLNN			
Systematic Error	**Random Error**	**Accuracy (%)**	**Precision**	**Recall**	**F1-score**
0	0 Mean ±0.104 SD	97.75 ± 0.00	0.9798	0.9825	0.9829
0 Mean ± 0.1SD		94.52 ± 0.62	0.9480	0.9459	0.9467
±1		92.21 ± 0.91	0.9256	0.9288	0.9269
±2		89.91 ± 1.01	0.8932	0.8998	0.8962
±3		87.22 ± 1.61	0.8752	0.8710	0.8733

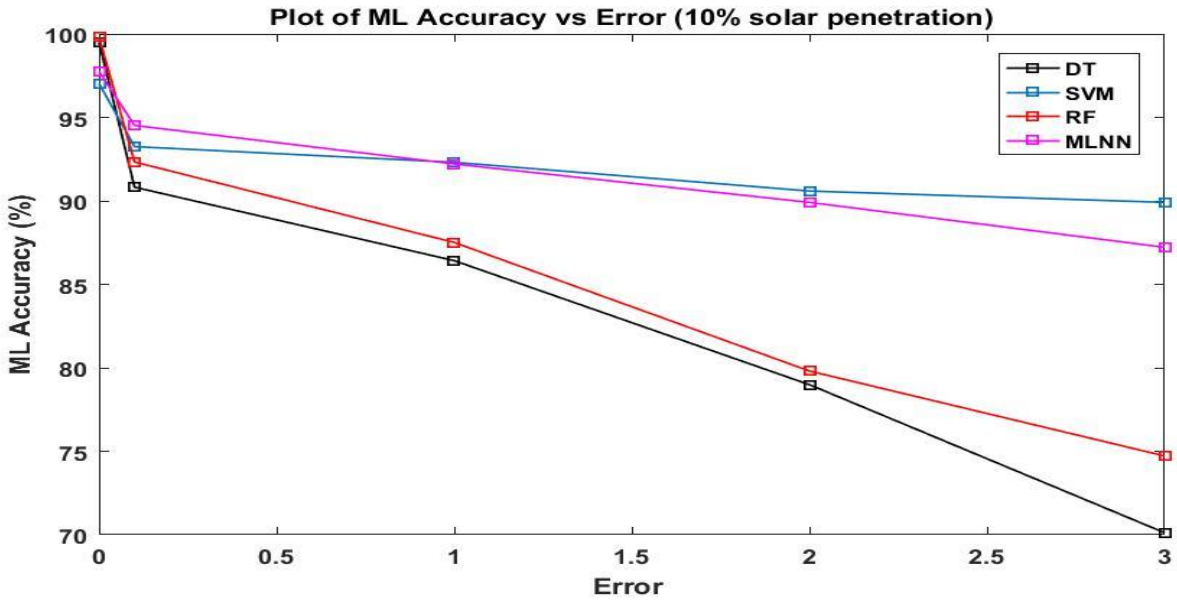

Figure 4. 27 Plot of ML Accuracy vs Error for 10% solar penetration

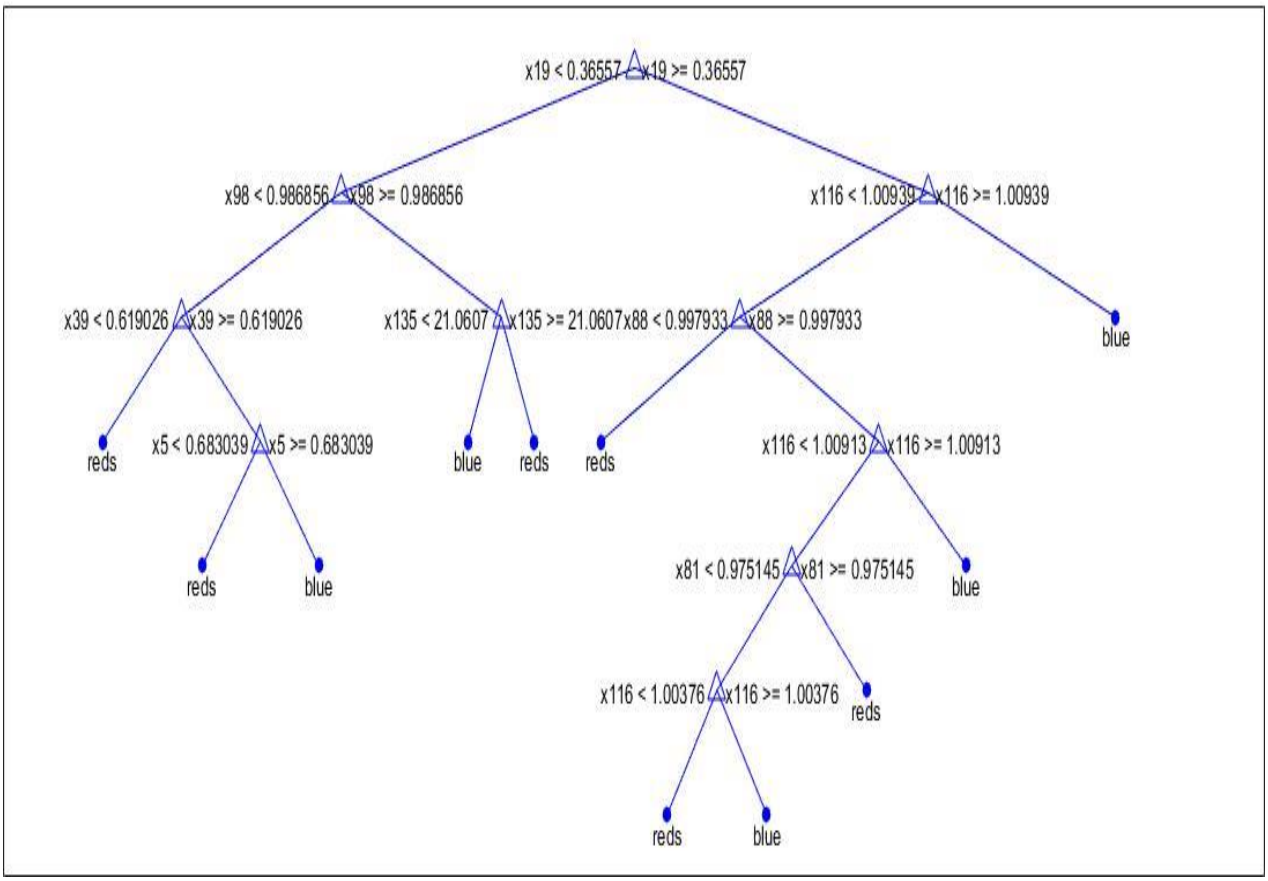

Figure 4. 28 DT results for 10% solar penetration

From the above tables (Tables 4.19-4.22) and Fig. 4.27 we arrive at the conclusion that for 10% solar penetration the performance of RF is better than other algorithms closely followed by DT without the addition of errors. With the addition of errors, SVM has the highest accuracy and its performance is better than all the other algorithms. Fig. 4.28, represents the DT results for 10% solar penetration where the "blue" terminal nodes indicate secure and "reds" terminal nodes indicate insecure points.

4.7.8 Results for 20% Solar Penetration Case:

Approximately 20% of the total generation is replaced with solar PV and the accuracy of the scheme is tested on this modified system. The simulations were repeated 75 times and a 95% confidence interval accuracy was computed for the test data with a range of measurement errors. The results obtained are presented below:

Table 4. 23 Summary of results for DT testing accuracies considering 20% solar penetration and measurement errors

Error		**DT**
Systematic Error	**Random Error**	**Accuracy (%)**
0	0 Mean ±0.104SD	99.69±0.00
0 Mean ± 0.1SD		92.03±0.67
±1		86.32±0.89
±2		77.46±1.99
±3		71.22±2.08

Table 4. 24 Summary of results for SVM testing accuracies for 20% solar penetration and considering measurement errors

Error		SVM			
Systematic Error	**Random Error**	**Accuracy (%)**	**Precision**	**Recall**	**F1-score**
0	0 Mean ±0.104 SD	96.89 ± 0.00	0.9708	0.9675	0.9689
0 Mean ± 0.1SD		93.42 ± 0.78	0.9734	0.9689	0.9625
±1		91.52 ± 0.92	0.9140	0.9165	0.9154
±2		90.59 ± 1.35	0.9030	0.9012	0.9018
±3		90.01 ± 1.61	0.9075	0.9021	0.9063

Table 4. 25 Summary of results for RF testing accuracies for 20% solar penetration and considering measurement errors

Error		RF			
Systematic Error	**Random Error**	**Accuracy (%)**	**Precision**	**Recall**	**F1-score**
0	0 Mean ±0.104 SD	99.74 ± 0.00	0.9998	0.9975	0.9990
0 Mean ± 0.1SD		92.98 ± 0.44	0.9234	0.9280	0.9210
±1		86.92 ± 0.81	0.8678	0.8610	0.8628
±2		80.05 ± 1.22	0.8001	0.8061	0.8034
±3		73.99 ± 1.82	0.7340	0.7380	0.7362

Table 4. 26 Summary of results for MLNN testing accuracies for 20% solar penetration and considering measurement errors

Error		MLNN			
Systematic Error	**Random Error**	**Accuracy (%)**	**Precision**	**Recall**	**F1-score**
0	0 Mean ±0.104 SD	97.80 ± 0.00	0.9798	0.9825	0.9820
0 Mean ± 0.1SD		93.10 ± 0.80	0.9346	0.9367	0.9352
±1		90.01 ± 1.10	0.9019	0.9055	0.9028
±2		89.32 ± 1.38	0.8920	0.8951	0.8935
±3		86.51 ± 1.82	0.8671	0.8600	0.8635

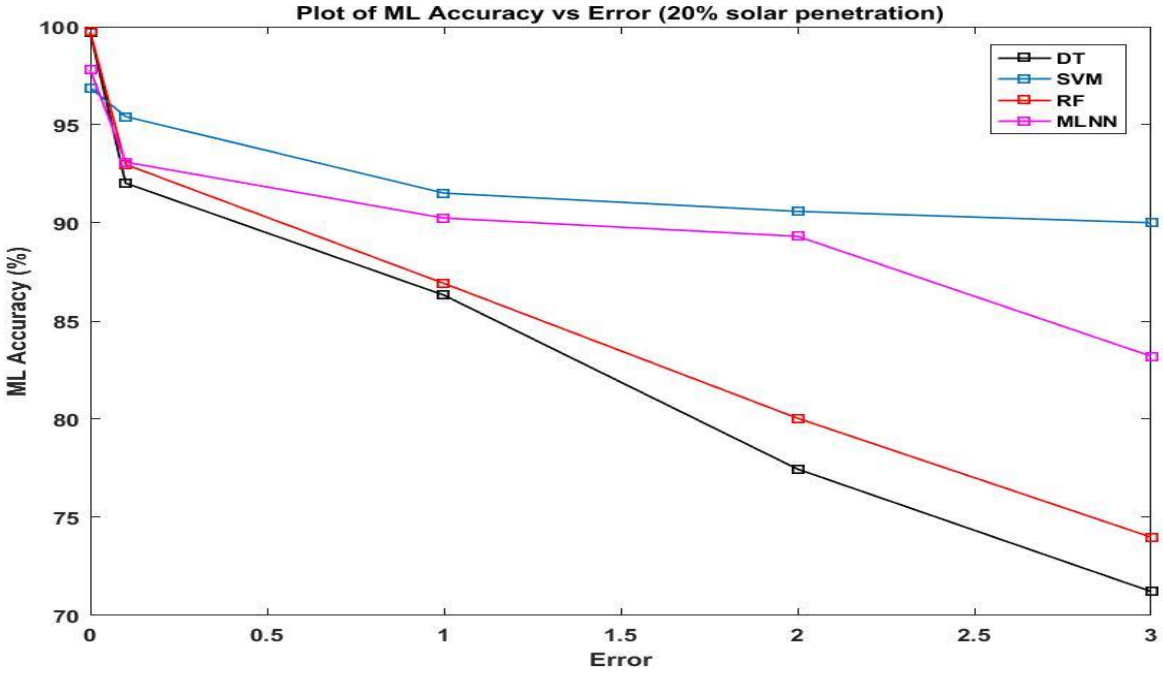

Figure 4. 29 Plot of ML Accuracy vs Error for 10% solar penetration

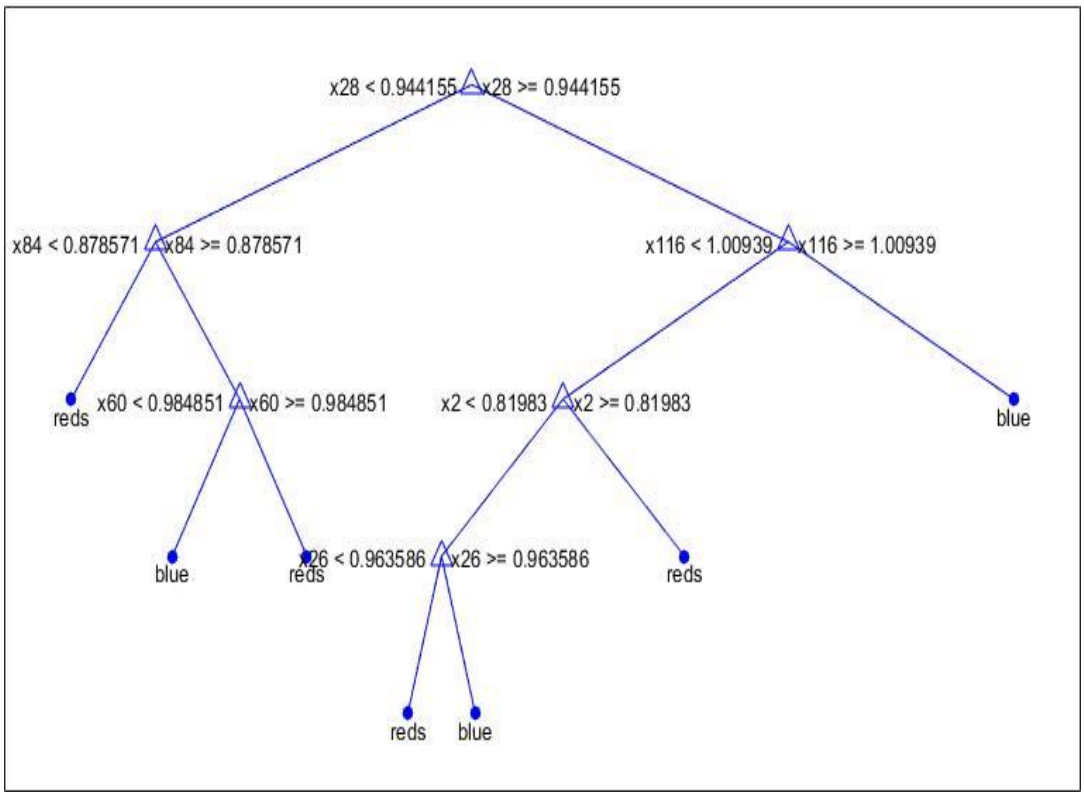

Figure 4. 30 DT results for 20% solar penetration

From the above tables (Tables 4.23-4.26) and Fig. 4.29 we arrive at the conclusion that for 20% solar penetration the performance of RF has been better than other algorithms without the presence of errors. With the addition of errors, SVM has the highest accuracy and its performance is better than all the other algorithms. Fig. 4.30, represents the DT results for 20% solar penetration wherein the “blue” terminal nodes indicate secure and “reds” terminal nodes indicate insecure points.

The results that have been tabulated above shows the classifying accuracy for the various ML algorithms with and without the addition of errors. The ML algorithms have been tested across various seasonal load profile as well as with the integration of solar PV in the grid. The importance of performing a seasonal based load modeling have been studied. Furthermore the significance of solar integration while performing a DSA scheme has also been discussed.

CHAPTER 5

5. CONCLUSION AND FUTURE SCOPE OF WORK

5.1 Discussion and Conclusion

In this thesis, a Dynamic Security Assessment (DSA) scheme has been developed considering different load variations corresponding to different seasons as well as varying amounts of solar penetration. Different machine learning (ML) techniques have been employed, such as decision trees (DTs), support vector machines (SVMs), random forests (RFs), and multi-layer neural networks (MLNNs), to classify the security of the system under different conditions. The following conclusions can be drawn from the study:

- The proposed scheme of using seasonal load has proved that under the same set of contingencies for a different season, the number of violations differ. Therefore, there is a need to include seasonal variability while doing DSA.
- With the inclusion of renewables in the study, for the same contingency scenarios, variations in transient stability and voltage security violations arise for systems which have renewable penetration and for systems having only conventional generation. Thus, renewable penetration must be taken into account while performing DSA.
- The performance of RF was found to be the best among all algorithms when measurement errors were not considered in the study.
- Substantial degradation in performance of RF was observed when measurement errors were introduced into the system.
- The performance of SVM was better than the other algorithms considered in the study when measurement errors were fed into the testing models.

5.2 Future Work

During the course of this research work we came across the following scopes that can be explored as future work:

- Incorporation of future projected loads into the study: Effect of loads that will scale up in the future can be incorporated into the study to make the load change more dynamic in nature. Regression based algorithms can be implemented to find the predicted load curves based on past historical data. EMS data which is available online can be utilized to project future loads to provide more flexibility to the proposed DSA scheme.
- Different types of faults at varying lengths of transmission line can be incorporated to create a varied range of contingency scenarios.
- Ensemble Learning Technique: Use of Ensemble learning techniques can be incorporated into the study for better classification accuracy.
- Application of a hybrid renewable generation scheme can be modeled and investigated.

REFERENCES

[1] U.S.-Canada Power System Outage Task Force, “Final Report on the August 14, 2003 Blackout in the United States and Canada: Causes and Recommendations,” U.S. Department of Energy, Washington DC, USA, Tech. Rep. April, 2004.

[2] European Commission, “A Roadmap for moving to a competitive low carbon economy in 2050,” 2011.

[3] P. Zhang, F. Li and N. Bhatt, "Next-Generation Monitoring, Analysis, and Control for the Future Smart Control Center," in *IEEE Transactions on Smart Grid*, vol. 1, no. 2, pp. 186-192, Sept. 2010.

[4] A. Phadke and J. Thorp, Synchronized Phasor Measurements and Their Applications. Springer Verlag, 2008

[5] A. Phadke, J. Thorp, and M. Adamiak, “A New Measurement Technique for Tracking Voltage Phasors, Local System Frequency, and Rate of Change of Frequency,” IEEE Transactions on Power Apparatus and Systems, vol. 102, no. 5, pp. 1025–1038, May 1983.

[6] V. Terzija *et al.*, "Wide-Area Monitoring, Protection, and Control of Future Electric Power Networks," in *Proceedings of the IEEE*, vol. 99, no. 1, pp. 80-93, Jan. 2011.

[7] H. Wu, Q. Wang and X. Li, "PMU-Based Wide Area Damping Control of Power Systems," *2008 Joint International Conference on Power System Technology and IEEE Power India Conference*, New Delhi, 2008, pp. 1-4.

[8] I. Kamwa, R. Grondin and Y. Hebert, "Wide-area measurement based stabilizing control of large power systems-a decentralized/hierarchical approach," in *IEEE Transactions on Power Systems*, vol. 16, no. 1, pp. 136-153, Feb 2001.

[9] P. Kundur et al., "Definition and classification of power system stability IEEE/CIGRE joint task force on stability terms and definitions," in IEEE Transactions on Power Systems, vol. 19, no. 3, pp. 1387-1401, Aug. 2004.

[10] Nerc planning standards (1997, sept.)...” http://www.nerc.com/~filez/pss-psg.html. Accessed: 2017-34-19.

[11] K. Morison, L. Wang, and P. Kundur, “Power system security assessment,” IEEE Power and Energy Magazine, vol. 2, October, pp. 30–39, 2004.

[12] Working Group Cigré C4.601, “Review of on-line dynamic security assessment tools and techniques,” 2007.

[13] S. C. Savulescu, Real-Time Stability Assessment in Modern Power System Control Centers. Wiley, 2008.

[14] "IEEE standard for synchrophasor measurements for power systems," IEEE Std 37.118.1-2011 (Revision of IEEE Std C37.118-2005), pp. 1–61, Dec 2011.

[15] M. Ghamsari-Yazdel, M. Esmaili, F. Aminifar, P. Gupta, A. Pal and H. Shayanfar, "Incorporation of Controlled Islanding Scenarios and Complex Substations in Optimal WAMS Design," in *IEEE Transactions on Power Systems*.

[16] A. Pal, G. A. Sánchez-Ayala, J. S. Thorp & V. A. Centeno (2016) A Community-based Partitioning Approach for Phasor Measurement Unit Placement in Large Systems, Electric Power Components and Systems, 44:12, 1317-1329.

[17] A. Pal, P. Chatterjee, J. S. Thorp and V. A. Centeno, "Online Calibration of Voltage Transformers Using Synchrophasor Measurements," in *IEEE Transactions on Power Delivery*, vol. 31, no. 1, pp. 370-380, Feb. 2016.

[18] F. Gao, J. S. Thorp, S. Gao, A. Pal & K. A. Vance (2015) A Voltage Phasor Based Fault-classification Method for Phasor Measurement Unit Only State Estimator Output, Electric Power Components and Systems, 43:1, 22-31.

[19] M. Li, A. Pal, A. G. Phadke, and J. S. Thorp, "Transient stability prediction based on apparent impedance trajectory recorded by PMUs," Int. J. Elect. Power Energy Syst., vol. 54, pp. 498-504, Jan. 2014.

[20] A. Pal, J. S. Thorp, S. S. Veda, and V. A. Centeno, "Applying a robust control technique to damp low frequency oscillations in the WECC," Int. J. Elect. Power Energy Syst., vol. 44, no. 1, pp. 638-645, Jan. 2013.

[21] https://www.energy.gov/sites/prod/files/2017/09/f36/2_Modern%20Gridnetworked%20Measurement%20and%20Monitoring%20Panel%20%20Alison%20Silverstein%2C%20NASPI.pdf

[22] G. S. Vassell, "Northeast Blackout of 1965," in *IEEE Power Engineering Review*, vol. 11, no. 1, pp. 4-, January 1991.

[23] L. Wang, X. Lin, F. Howell, K. Morison, (2014) Practical Issues for Implementation of Online Dynamic Security Assessment Systems. In: Savulescu S. (eds) Real-Time Stability in Power Systems. Power Electronics and Power Systems. Springer, Cham

[24] G. C. Ejebe *et al.*, "Online dynamic security assessment in an EMS," in *IEEE Computer Applications in Power*, vol. 11, no. 1, pp. 43-47, Jan. 1998.

[25] J. Tong and L. Wang, "Design of a DSA Tool for Real Time System Operations," *2006 International Conference on Power System Technology*, Chongqing, 2006, pp. 1-5.

[26] L. Yan, C. YangQuan, P. Igor, Stability of fractional-order nonlinear dynamic systems: Lyapunov direct method and generalized Mittag–Leffler stability, Computers & Mathematics with Applications, Volume 59, Issue 5 ,2010, Pages 1810-1821.

[27] T. Athay, R. Podmore and S. Virmani, "A Practical Method for the Direct Analysis of Transient Stability," in *IEEE Transactions on Power Apparatus and Systems*, vol. PAS-98, no. 2, pp. 573-584, March 1979.

[28] A. A. Fouad, V. Vittal and T. K. Oh, "Critical Energy for Direct Transient Stability Assessment of a Multimachine Power System," in *IEEE Transactions on Power Apparatus and Systems*, vol. PAS-103, no. 8, pp. 2199-2206, Aug. 1984.

[29] Y. Xue, T. Van Cutsem and M. Ribbens-Pavella, "A simple direct method for fast transient stability assessment of large power systems," in *IEEE Transactions on Power Systems*, vol. 3, no. 2, pp. 400-412, May 1988.

[30] K. Khorasani, M.A. Pai, P.W. Sauer, Modal based stability analysis of power systems using energy functions, International Journal of Electrical Power & Energy Systems, Volume 8, Issue 1,1986.

[31] H. Chiang, J. Tong and Y. Tada, "On-line transient stability screening of 14,000-bus models using TEPCO-BCU: Evaluations and methods," *IEEE PES General Meeting*, Providence, RI, 2010, pp. 1-8.

[32] A. Jain and N. R. Shivakumar, "Power system tracking and dynamic state estimation," *2009 IEEE/PES Power Systems Conference and Exposition*, Seattle, WA, 2009, pp. 1-8.

[33] G. Valverde, V. Terzija,'Unscented Kalman filter for power system dynamic state estimation', IET Generation, Transmission & Distribution, 2011, 5, (1), p. 29-37.

[34] L. Yanli, Y. Ziyuan, Y. Yixin, An Analytical Approach to Probabilistic Dynamic Security Assessment of Power Systems Incorporating Wind Farms, Energy Procedia, Volume 142,2017,Pages 224-229.

[35] A. Dissanayaka, U. D. Annakkage, B. Jayasekara and B. Bagen, "Risk-Based Dynamic Security Assessment," in *IEEE Transactions on Power Systems*, vol. 26, no. 3, pp. 1302-1308, Aug. 2011.

[36] N. Balu *et al.*, "On-line power system security analysis," in *Proceedings of the IEEE*, vol. 80, no. 2, pp. 262-282, Feb. 1992.

[37] J. A. Huang *et al*., "An intelligent system for advanced dynamic security assessment," *Proceedings. International Conference on Power System Technology*, Kunming, China, 2002, pp. 220-224 vol.1.

[38] Y. Xu, Z. Y. Dong, Z. Xu, K. Meng and K. P. Wong, "An Intelligent Dynamic Security Assessment Framework for Power Systems With Wind Power," in *IEEE Transactions on Industrial Informatics*, vol. 8, no. 4, pp. 995-1003, Nov. 2012.

[39] K. Sun, S. Likhate, V. Vittal, V. S. Kolluri and S. Mandal, "An Online Dynamic Security Assessment Scheme Using Phasor Measurements and Decision Trees," in *IEEE Transactions on Power Systems*, vol. 22, no. 4, pp. 1935-1943, Nov. 2007.

[40] I. Genc, R. Diao, V. Vittal, S. Kolluri and S. Mandal, "Decision Tree-Based Preventive and Corrective Control Applications for Dynamic Security Enhancement in Power Systems," in *IEEE Transactions on Power Systems*, vol. 25, no. 3, pp. 1611-1619, Aug. 2010.

[41] N. Wahab, A. Mohamed and A. Hussain, 2007. Transient Stability Assessment of a Power System Using PNN and LS-SVM Methods. Journal of Applied Sciences.

[42] S. Kalyani and K. S. Swarup, "Binary SVM Approach for Security Assessment and Classification in Power Systems," *2009 Annual IEEE India Conference*, Gujarat, 2009, pp. 1-4.

[43] Y. Xu, Z. Y. Dong, J. H. Zhao, P. Zhang and K. P. Wong, "A Reliable Intelligent System for Real-Time Dynamic Security Assessment of Power Systems," in *IEEE Transactions on Power Systems*, vol. 27, no. 3, pp. 1253-1263, Aug. 2012.

[44] Liu et al., "An Accurate Online Dynamic Security Assessment Scheme Based on Random Forest ", Electric Power and Energy Systems, MDPI.

[45] Working Group Cigré C4.601, "Review of on-line dynamic security assessment tools and techniques," 2007.

[46] A. Pal, A. K. S. Vullikanti, and S. S. Ravi, "A PMU placement scheme considering realistic costs and modern trends in relaying," IEEE Trans. Power Syst., vol. 32, no. 1, pp. 552-561, Jan. 2017.

[47] A. Pal, C. Mishra, A. K. S. Vullikanti, and S. S. Ravi, "General optimal substation coverage algorithm for phasor measurement unit placement in practical systems," IET Gener., Transm. Distrib., vol. 11, no. 2, pp. 347-353, Jan. 2017.

[48] C. Mishra, K. D. Jones, A. Pal, and V. A. Centeno, "Binary particle swarm optimization based optimal substation coverage algorithm for phasor measurement unit installations in practical systems," IET Gener. Transm. Distrib., vol. 10, no. 2, pp. 555-562, Feb. 2016.

[49] A. Pal, G. A. Sanchez-Ayala, V. A. Centeno, and J. S. Thorp, “A pmu placement scheme ensuring real-time monitoring of critical buses of the network,” IEEE Transactions on Power Delivery, vol. 29, pp. 510–517, April 2014.

[50] P. M. Anderson and A. A. Fouad, Power System Control and Stability, 2nd ed. New York: IEEE Press, 2003.

[51] http://cigre-usnc.tamu.edu/wp-content/uploads/2016/10/Wang.pdf

[52] https://www.dsatools.com/tsat/

[53] C. Liu et al., "A Systematic Approach for Dynamic Security Assessment and the Corresponding Preventive Control Scheme Based on Decision Trees," in IEEE Transactions on Power Systems, vol. 29, no. 2, pp. 717-730, March 2014.

[54] R. Diao *et al*., "Decision Tree-Based Online Voltage Security Assessment Using PMU Measurements," in *IEEE Transactions on Power Systems*, vol. 24, no. 2, pp. 832-839, May 2009.

[55] M. He, V. Vittal and J. Zhang, "Online dynamic security assessment with missing pmu measurements: A data mining approach," in *IEEE Transactions on Power Systems*, vol. 28, no. 2, pp. 1969-1977, May 2013.

[56] T. Wang, A. Pal, J. S. Thorp, Z. Wang, J. Liu, and Y. Yang, “Multi-polytope based adaptive robust damping control in power systems using CART,” IEEE Trans. Power Syst., vol. 30, no. 4, pp. 2063-2072, Jul. 2015.

[57] A. Pal, J. S. Thorp, T. Khan, and S. S. Young, “Classification trees for complex synchrophasor data,” Elect. Power Compon. Syst., vol. 41, no. 14, pp. 1381-1396, Sep. 2013.

[58] L. Breiman, J. H. Friedman, R. Olshen, and C. J. Stone, Classification and Regression Tree, Wadsworth & Brooks/Cole Advanced Books & Software, Pacific California, 1984.

[59] Tin Kam Ho, "Random decision forests," *Proceedings of 3rd International Conference on Document Analysis and Recognition*, Montreal, Quebec, Canada, 1995, pp. 278-282 vol.1.

[60] P. Sekhar, and S. Mohanty, (2016) Classification and assessment of power system static security using decision tree and random forest classifiers. Int. J. Numer. Model. 29: 465– 474.

[61] M. Negnevitsky, N. Tomin, V. Kurbatsky, D. Panasetsky, A. Zhukov and C. Rehtanz, "A random forest-based approach for voltage security monitoring in a power system," *2015 IEEE Eindhoven PowerTech*, Eindhoven, 2015, pp. 1-6.

[62] J. Zhou, Z. Ge, S. Gao and Y. Xu, "Fault record detection with random forests in data center of large power grid," *2016 IEEE PES Asia-Pacific Power and Energy Engineering Conference (APPEEC)*, Xi'an, 2016, pp. 1641-1645.

[63] A. Lahouar, A. Mejri and J. Ben Hadj Slama, "Importance based selection method for day-ahead photovoltaic power forecast using random forests," *2017 International Conference on Green Energy Conversion Systems (GECS)*, Hammamet, 2017, pp. 1-7.

[64] Fei Tang et al. "An Accurate Online Dynamic Security Assessment Scheme." Energies 11.7 (2018): 1914

[65] Breiman, L. Random forest. Mach. Learn. 2001, 45, 5–32

[66] V. Vapnik, Statistical Learning Theory. New York: Wiley, 1998.

[67] Z. Yun, Q. Zhou, Y. Feng, D. Sun, J. Sun and D. Yang, "On-line static voltage security risk assessment based on Markov chain model and SVM for wind integrated power system," *2017 13th International Conference on Natural Computation, Fuzzy Systems and Knowledge Discovery (ICNC-FSKD)*, Guilin, 2017, pp. 2469-2473.

[68] Z. Zhao, Y. Lou, J. Ni and J. Zhang, "RBF-SVM and its application on reliability evaluation of electric power system communication network," *2009 International Conference on Machine Learning and Cybernetics*, Hebei, 2009, pp. 1188-1193.

[69] N. Tomin, V. Kurbatsky and C. Rehtanz, "An intelligent security alert system for power system pre-emergency control," *2013 13th International Conference on Environment and Electrical Engineering (EEEIC)*, Wroclaw, 2013, pp. 63-67.

[70] X. Meng, G. Sun, J. Li and H. Liu, "Automatic reactive power and voltage control for regional power grid based on SVM," *2013 IEEE International Conference of IEEE Region 10 (TENCON 2013)*, Xi'an, 2013, pp. 1-4.

[71] S. Kamalasadan, G. D. Swann and R. Yousefian, "A Novel System-Centric Intelligent Adaptive Control Architecture for Power System Stabilizer Based on Adaptive Neural Networks," in *IEEE Systems Journal*, vol. 8, no. 4, pp. 1074-1085, Dec. 2014.

[72] M. C. Su, C. Liu and S. Tsay, "Neural-network-based fuzzy model and its application to transient stability prediction in power systems," in *IEEE Transactions on Systems, Man, and Cybernetics, Part C (Applications and Reviews)*, vol. 29, no. 1, pp. 149-157, Feb. 1999.

[73] Y. Han, L. Xiu, Z. Wang, Q. Chen and S. Tan, "Artificial neural networks controlled fast valving in a power generation plant," in *IEEE Transactions on Neural Networks*, vol. 8, no. 2, pp. 373-389, March 1997.

[74] J. Knisley, L. Glenn, K. Joplin and P. Carey, Artificial Neural Networks for Data Mining and Feature Extraction, in Quantitative Medical Data Analysis Using Mathematical Tools and Statistical Techniques, eds. I. Stojmenovic and A. Nayak (World Scientific, 2006).

[75] "Multilayer feedforward networks are universal approximators" Kur Hornik, Maxwell Stinchcombe and Halber White(1989).

[76] https://en.wikipedia.org/wiki/Gradient_descent

[77] G. Klambauer, T. Unterthiner, A. Mayr, and S. Hochreiter, Self-normalizing neural networks. arXiv preprint arXiv:1706.02515, 2017

[78] "IEEE 118-bus system." http://icseg.iti.illinois.edu/ ieee-118-bus-system/. Accessed: 2017-3-25.

[79] https://www.caiso.com/Documents/HistoricalEMSHourlyLoadDataAvailable.html

[80] https://www.ferc.gov/industries/electric/indus-act/market-planning/opf-papers/acopf-1-historyformulation-testing.pdf

[81] "2016 state of the interconnection," tech. rep., WECC, 2016.

[82] http://www.caiso.com/TodaysOutlook/Pages/Supply.aspx

[83] https://www.nrel.gov/research/re-photovoltaics.html

[84] WECC Guide for Representation of Photovoltaic Systems in Large-Scale Load Flow Simulations, WECC Renewable Energy Modeling Task Force

[85] WECC Solar Power Plant Power Flow Modeling Guide", WECC Modeling and Validation Work Group, May 2008. [Online] Available: https://www.wecc.org/Reliability/WECC%20Solar%20Plant%20Dynamic%20Modeling%20Guidelines.pdf

[86] A. Pal, P. Chatterjee, J. S. Thorp, and V. A. Centeno, "On-line calibration of voltage transformers using synchrophasor measurements," IEEE Trans. Power Del., vol. 31, no. 1, pp. 370-380, Feb. 2016

[87] M. Asprou, S. Chakrabarti and E. Kyriakides, "A Two-Stage State Estimator for Dynamic Monitoring of Power Systems," in *IEEE Systems Journal*, vol. 11, no. 3, pp. 1767-1776, Sept. 2017.

[88] M. Asprou and E. Kyriakides, "Identification and Estimation of Erroneous Transmission Line Parameters Using PMU Measurements," in *IEEE Transactions on Power Delivery*, vol. 32, no. 6, pp. 2510-2519, Dec. 2017.